J. Mech. Phys. Solids 145 (2020) 104161

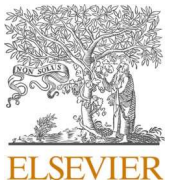

Contents lists available at ScienceDirect

Journal of the Mechanics and Physics of Solids

journal homepage: www.elsevier.com/locate/jmps

On the peridynamic effective force state and multiphase constitutive correspondence principle

Xiaoyu Song [a,*], Stewart A. Silling [b]

[a] Engineering School of Sustainable Infrastructure & Environment, University of Florida, Gainesville, Florida 32611 USA
[b] Computational Multiscale Department, Sandia National Laboratories, Albuquerque, New Mexico 87185 USA

ARTICLE INFO

Keywords:
Peridynamics
Unsaturated porous media
Thermodynamics
Effective force state
Multiphase correspondence principle

ABSTRACT

This article concerns modeling unsaturated deformable porous media as an equivalent single-phase and single-force state peridynamic material through the effective force state. The balance equations of linear momentum and mass of unsaturated porous media are presented by defining relevant peridynamic states. The energy balance of unsaturated porous media is utilized to derive the effective force state for the solid skeleton that is an energy conjugate to the nonlocal deformation state of the solid, and the suction force state. Through an energy equivalence, a multiphase constitutive correspondence principle is built between classical unsaturated poromechanics and peridynamic unsaturated poromechanics. The multiphase correspondence principle provides a means to incorporate advanced constitutive models in classical unsaturated porous theory directly into unsaturated peridynamic poromechanics. Numerical simulations of localized failure in unsaturated porous media under different matric suctions are presented to demonstrate the feasibility of modeling the mechanical behavior of such three-phase materials as an equivalent single-phase peridynamic material through the effective force state concept.

1. Introduction

Porous materials are classified as those with an internal structure, which comprise a solid phase and closed and/or open pores. Poromechanics studies porous materials whose mechanical behavior is significantly impacted by pore fluids (Coussy, 2004; Cowin and Doty, 2007; De Boer, 2000). Thus poromechanics deals with a broad range of materials from geological materials (i.e., soils and rocks) to gels and biological tissues (Dormieux et al., 2006; Ji and Gao, 2004). Porous media such as geological materials and human tissues (e.g., human bones) consist of a solid phase, usually referred to as a matrix or skeleton, and open-pore space filled with one or more types of fluids (e.g., wetting and non-wetting fluids). Mathematical modeling of such porous media is important in numerous fields of engineering and science (Coussy, 2011; Zienkiewicz et al., 1999). Classical poromechanics is formulated either based on the mixture theory (e.g., Biot, 1941; Bowen, 1982) with the volume fraction concept or the average theory (e.g., Gray and Miller, 2014; Gray et al., 2013) which are local theory. The mixture theory assumes porous media as the continuous medium at the macroscopic scale. Volume fractions are determined by the ratio of the constituents' volume to the volume of the mixture. The averaging theory starts at the microscale or pore scale and uses average operators to describe porous media's mechanical behavior. The field equations for porous media generated by both methods are the partial differential equations, e.g., the balance equations of linear momentum and mass (Lewis and Schrefler, 1998). While the partial differential equations are essential for describing the multi-physical behavior of

* Corresponding author.
E-mail address: xysong@ufl.edu (X. Song).

https://doi.org/10.1016/j.jmps.2020.104161
Received 28 July 2020; Received in revised form 7 September 2020; Accepted 20 September 2020
Available online 25 September 2020
0022-5096/

materials, they have difficulty in characterizing discontinuities in displacements or fluid pressures because of singularities at discontinuities (Stakgold and Holst, 2011). Advanced numerical techniques developed for modeling single-phase solid materials have been applied to simulate discontinuities like shear bands or cracks in porous media (see Lu and Mitchell, 2019, for a recent review on the subject). This article is focused on modeling unsaturated porous media through the state-based peridynamics, a strong nonlocal theory (Silling et al., 2007; Silling and Lehoucq, 2010). As a new contribution, in this article we derive the peridynamic effective force state and the multiphase constitutive correspondence principle through energy methods.

The state-based peridynamics which is generalized bond-based peridynamics (Silling, 2000) is a mathematical reformulation of classical solid mechanics for modeling continuous, discontinuous materials, and discontinuities (e.g., shear bands) within the same mathematical model. It achieves this goal by describing the mechanical behavior using integral/integral-differential equations instead of partial differential equations. Here integration is in space, and differentiation is in time. Peridynamics has been applied to model cracks, plastic or viscoplastic deformation, and atomistic to continuum coupling in single-phase solid materials (e.g., Bobaru et al., 2016; Foster et al., 2010; Gerstle et al., 2007; Lai et al., 2015; Madenci and Oterkus, 2013; Parks et al., 2008; Warren et al., 2009). Peridynamics has also been utilized to simulate pressure driven convective fluid transport in porous media (e.g., Jabakhanji and Mohtar, 2015; Katiyar et al., 2014) as well as poroelastic problems (e.g., Ouchi et al., 2015; Turner, 2013). Recently, peridynamics has been used to study the mechanical behavior of unsaturated geomaterials (e.g., Menon and Song, 2019; Song and Khalili, 2019; Song and Menon, 2018). For example, a pressure-sensitive elastoplastic model for unsaturated geomaterials Song and Khalili (2019) was formulated through the peridynamic correspondence principle for solid materials (Silling, 2017; Silling et al., 2007). It was demonstrated that peridynamics is a useful tool to model localized failure in unsaturated geomaterials. In those research and others for coupled poroelastic problems, the effective stress concept in classical unsaturated poromechanics (e.g., Borja, 2006; Houlsby, 1997; Khalili and Khabbaz, 1998; Lu, 2020; Lu et al., 2010; Lu and Likos, 2006; Nikooee et al., 2013; Nuth and Laloui, 2008) has been adopted to describe the force state of the solid skeleton without a thermodynamic justification in the framework of peridynamics.

Meanwhile, there is no thermodynamically consistent formulation for modeling unsaturated poromechanics problems through peridynamics in the literature. In this paper, the peridynamic linear momentum balance for unsaturated porous media is formulated by assuming a potential energy function. The mass balance equations for unsaturated porous media are formulated by defining peridynamic dilation states. Through reformulating the first law of thermodynamics for unsaturated porous media, we derive the effective force state of the solid skeleton and show that it is an energy conjugate to the nonlocal deformation state of the solid skeleton. Specifically, the effective force state derived is a function of the total force state of the mixture, the force states of pore fluids and their degrees of saturation, and the bulk modulus of the solid skeleton and the solid grains. The suction force state is defined as the difference between the pore air force state and the pore water force state. The second law of thermodynamics demonstrates that a free energy function can be applied to determine the effective force state for the solid skeleton, and provides the thermodynamic restrictions on constitutive and physical laws for modeling unsaturated porous media. Then the multiphase constitutive correspondence principle for unsaturated porous media is built between classical unsaturated poromechanics and peri-poromechanics to incorporate the classical constitutive theory in peri-poromechanics. Numerical examples are presented to demonstrate the feasibility of modeling unsaturated porous media as an equivalent single-phase and single-force state peridynamic material.

The remainder of the article is as follows. Section 2 presents the peridynamic balance equations of linear momentum and mass for unsaturated porous media. Section 3 deals with the effective force state for the solid skeleton and the energy conjugates and entropy restrictions on constitutive models. Section 4 concerns the multiphase constitutive correspondence principle for unsaturated peri-poromechanics. Section 5 presents numerical examples for modeling unsaturated porous media through the effective force state concept, followed by a summary in Section 6. Appendix A presents common peridynamic operators. Appendix B briefly reviews classical unsaturated poromechanics for deforming unsaturated porous media. For sign convention, force states (or stress) for the solid skeleton, pore fluids, and the mixture are positive in tension, and pressures for pore fluids are positive in compression.

2. Peridynamic balance equations for unsaturated porous media

In this section, the peridynamic governing equations of unsaturated porous media are formulated through peridynamic state concept, which will be used to derive the perdynamic effective force state for the solid skeleton in the next section. In this formulation, it is assumed that (i) the porous media are composed of material points that interact with each other within a finite distance, (ii) the porous medium is considered as the superposition of a solid skeleton and two pore fluids (water and air) that move with distinct kinematics, while mechanically interacting and exchanging energy and matter, and (iii) the equations governing the physics of the superposed fluid and solid continua from their common current configuration are transported to an initial reference configuration related to the solid skeleton in that the formulation of constitutive equations for a solid material is usually referred to its initial configuration. Thus, each material point has five degrees of freedom, i.e., three for displacement and two for pore fluid pressures. In line with the classic unsaturated poromechanics, the solid skeleton is described by the Lagrangian coordinate system, and pore fluids are described by the relative Eulerian coordinate system with respect to the solid skeleton.

2.1. Peridynamic states

In the state-based peridynamics theory, mathematical objects called peridynamic states are introduced. For the sake of completeness, the peridynamic states are briefly reviewed. Peridynamic states depend upon position and time and operate on a vector connecting any two material points. Depending on whether the value of this operation is a scalar or vector, the peridynamic state is called a scalar state or a vector state. The mapping defined by peridynamic states provide the fundamental objects on which

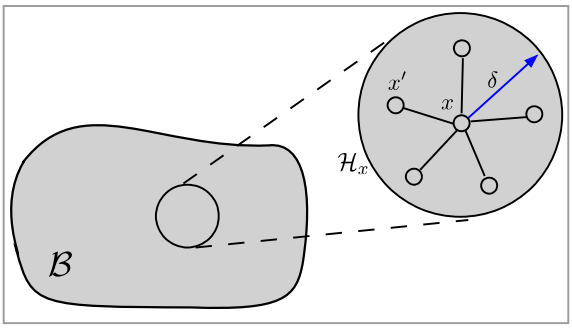

Fig. 1. The family $\mathcal{H}$ contains the relative position vectors (bonds) connecting $\boldsymbol{x}$ to points such as $\boldsymbol{x}'$ within a distance δ of $\boldsymbol{x}$.

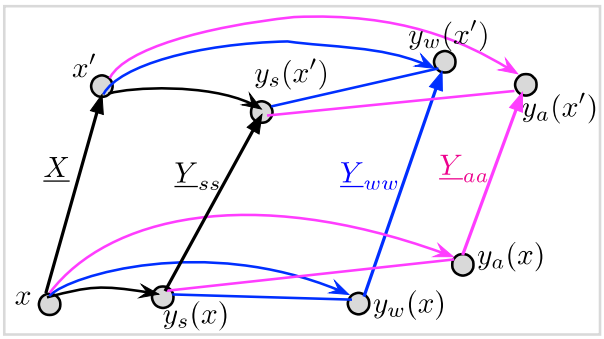

Fig. 2. Schematic of kinematics of three phase porous media in peri-poromechanics.

constitutive models operate in the nonlocal setting of peridynamics. Consider a body $\mathcal{B}$. Let δ be a positive number, called the *horizon*. For a given $\boldsymbol{x} \in \mathcal{B}$, let $\mathcal{H}_x$ be a neighborhood of radius δ centered at $\boldsymbol{X}$, as shown in as shown in Fig. 1.

Define the *family* of $\boldsymbol{x}$ by

$$\mathcal{H} = \{\boldsymbol{\xi} \in (\mathbb{R}^3 \setminus \boldsymbol{0}) | (\boldsymbol{\xi} + \boldsymbol{x}) \in (\mathcal{H}_x \cap \mathcal{B})\}. \tag{1}$$

A peridynamic *state* $\underline{\mathrm{A}}\langle \cdot \rangle$ is a function on $\mathcal{H}$. The angle brackets enclose the bond vector, and parentheses and square brackets indicate dependencies of the state on other quantities. It is noted that a peridynamic state need not be a differentiable or continuous function of the bonds in $\mathcal{H}$. In the following formulation, peridynamic states will be defined in the order of their first appearance. For brevity, the square bracket and angle bracket may be omitted if not causing confusion.

The family of a point is a nonlocal interaction region for the point in the bulk. The region is commonly assumed to be of spherical or circular shape. The radius of the horizon region is referred to as the horizon size or simply the horizon. The peridynamic nonlocal interaction does not necessarily mean or refer to the nonlocal physical direct interaction that does exist between atoms and molecule (Silling et al., 2015; Silling, 2014; Song and Wang, 2019). The peridynamic horizon may be viewed as an "effective interaction distance" or "effective length scale" of a continuum model in a dynamic problem (Bobaru and Hu, 2012). The horizon can also be matched to the dominant length scale of material inhomogeneities, enabling multiscale modeling for complex materials. For instance, it was demonstrated in Song and Khalili (2019) that the horizon can be utilized to model the thickness of shear bands in geomaterials (Sulem and Vardoulakis, 1995).

2.2. Balance of linear momentum of unsaturated porous media

The medium is assumed to consist of three phases, denoted by *s*, *w*, and *a* for the solid skeleton, pore water, and pore air, respectively. The deformation positions of a point $\boldsymbol{x}$ for all phases are $\boldsymbol{y}_s(\boldsymbol{x})$, $\boldsymbol{y}_w(\boldsymbol{x})$, and $\boldsymbol{y}_a(\boldsymbol{x})$. Fig. 2 shows the peridynamic kinematics of three-phase porous media. Referring to Fig. 2 and ignoring the relative deformation states between porous fluid phases, we define the multiphase deformation states for each phase and the relative deformation states between the solid phase and the pore fluid phase as follows,

$$\underline{\boldsymbol{Y}}_{ss}[\boldsymbol{x}]\langle \boldsymbol{x}' - \boldsymbol{x} \rangle = \boldsymbol{y}_s(\boldsymbol{x}') - \boldsymbol{y}_s(\boldsymbol{x}), \tag{2}$$

$$\underline{\boldsymbol{Y}}_{ww}[\boldsymbol{x}]\langle \boldsymbol{x}' - \boldsymbol{x} \rangle = \boldsymbol{y}_w(\boldsymbol{x}') - \boldsymbol{y}_w(\boldsymbol{x}), \tag{3}$$

$$\underline{\boldsymbol{Y}}_{aa}[\boldsymbol{x}]\langle \boldsymbol{x}' - \boldsymbol{x}\rangle = \boldsymbol{y}_a(\boldsymbol{x}') - \boldsymbol{y}_a(\boldsymbol{x}), \tag{4}$$

$$\underline{\boldsymbol{Y}}_{sw}[\boldsymbol{x}]\langle \boldsymbol{x}' - \boldsymbol{x}\rangle = \boldsymbol{y}_s(\boldsymbol{x}') - \boldsymbol{y}_w(\boldsymbol{x}), \tag{5}$$

$$\underline{\boldsymbol{Y}}_{ws}[\boldsymbol{x}]\langle \boldsymbol{x}' - \boldsymbol{x}\rangle = \boldsymbol{y}_w(\boldsymbol{x}') - \boldsymbol{y}_s(\boldsymbol{x}), \tag{6}$$

$$\underline{\boldsymbol{Y}}_{sa}[\boldsymbol{x}]\langle \boldsymbol{x}' - \boldsymbol{x}\rangle = \boldsymbol{y}_s(\boldsymbol{x}') - \boldsymbol{y}_a(\boldsymbol{x}), \tag{7}$$

$$\underline{\boldsymbol{Y}}_{as}[\boldsymbol{x}]\langle \boldsymbol{x}' - \boldsymbol{x}\rangle = \boldsymbol{y}_a(\boldsymbol{x}') - \boldsymbol{y}_s(\boldsymbol{x}), \tag{8}$$

Without of loss of generality we assume there is no interaction between pore water and pore air. Suppose there is a free energy density for the three-phase mixture as

$$W\left(\underline{\boldsymbol{Y}}_{ss}, \underline{\boldsymbol{Y}}_{ww}, \underline{\boldsymbol{Y}}_{aa}, \underline{\boldsymbol{Y}}_{sw}, \underline{\boldsymbol{Y}}_{ws}, \underline{\boldsymbol{Y}}_{sa}, \underline{\boldsymbol{Y}}_{as}\right) \tag{9}$$

The total potential energy in a bounded body $\mathcal{B}$ is given by

$$\tilde{W} = \int_{\mathcal{B}} \left(W(\boldsymbol{x}) - \boldsymbol{b}_s(\boldsymbol{x}) \cdot \boldsymbol{y}_s(\boldsymbol{x}) - \boldsymbol{b}_w(\boldsymbol{x}) \cdot \boldsymbol{y}_w(\boldsymbol{x}) - \boldsymbol{b}_a(\boldsymbol{x}) \cdot \boldsymbol{y}_a(\boldsymbol{x}) \right) \mathrm{d}V, \tag{10}$$

where $\boldsymbol{b}_s(\boldsymbol{x})$, $\boldsymbol{b}_w(\boldsymbol{x})$, and $\boldsymbol{b}_a(\boldsymbol{x})$ are body forces of the solid skeleton, pore water and pore air, respectively. The Fréchet derivatives of W supply the material model for bonds within or between the phases, which are denoted by

$$\underline{\boldsymbol{T}}_{\alpha\beta} = \frac{\partial W}{\partial \underline{\boldsymbol{Y}}_{\alpha\beta}}, \tag{11}$$

where $\alpha = s, w, a$, and $\beta = s, w, a$. By the properties of Fréchet derivatives, small changes $\Delta \boldsymbol{y}_\alpha$ near $\boldsymbol{x}$ result in the following changes in W at $\boldsymbol{x}$:

$$\Delta W = \sum_{\alpha=s,w,a} \underline{\boldsymbol{T}}_{a\alpha} \bullet \Delta \underline{\boldsymbol{Y}}_{a\alpha} + \sum_{\alpha=w,a} \left(\underline{\boldsymbol{T}}_{s\alpha} \bullet \Delta \underline{\boldsymbol{Y}}_{s\alpha} + \underline{\boldsymbol{T}}_{as} \bullet \Delta \underline{\boldsymbol{Y}}_{as} \right). \tag{12}$$

where the dot product of two vector states is defined in Appendix A. To derive the equilibrium equation for the solid phase, take the first variation of $\tilde{W}$ with respect to $\underline{\boldsymbol{Y}}_{\alpha\alpha}$ with $\alpha = s, w, a$ and set to 0:

$$\begin{aligned} 0 = & \int_{\mathcal{B}} \left[\sum_{\alpha=s,w,a} \underline{\boldsymbol{T}}_{a\alpha} \bullet \Delta \underline{\boldsymbol{Y}}_{a\alpha} + \sum_{\alpha=w,a} \left(\underline{\boldsymbol{T}}_{s\alpha} \bullet \Delta \underline{\boldsymbol{Y}}_{s\alpha} + \underline{\boldsymbol{T}}_{as} \bullet \Delta \underline{\boldsymbol{Y}}_{as} \right) - \sum_{\alpha=s,w,a} \boldsymbol{b}_\alpha \Delta \boldsymbol{y}_\alpha \right] \mathrm{d}V \\ = & \int_{\mathcal{B}} \left\{ \int_{\mathcal{H}} \left[\sum_{\alpha=s,w,a} \underline{\boldsymbol{T}}_{a\alpha}[\boldsymbol{x}]\langle \boldsymbol{x}' - \boldsymbol{x}\rangle \cdot (\Delta \boldsymbol{y}_\alpha(\boldsymbol{x}') - \Delta \boldsymbol{y}_\alpha(\boldsymbol{x})) \right. \right. \\ & \left. + \sum_{\alpha=w,a} \left(\underline{\boldsymbol{T}}_{s\alpha}[\boldsymbol{x}]\langle \boldsymbol{x}' - \boldsymbol{x}\rangle \cdot (\Delta \boldsymbol{y}_s(\boldsymbol{x}') - \Delta \boldsymbol{y}_\alpha(\boldsymbol{x})) + \underline{\boldsymbol{T}}_{as}[\boldsymbol{x}]\langle \boldsymbol{x}' - \boldsymbol{x}\rangle \cdot (\Delta \boldsymbol{y}_\alpha(\boldsymbol{x}') - \Delta \boldsymbol{y}_s(\boldsymbol{x})) \right) \right] \mathrm{d}V' \\ & \left. - \sum_{\alpha=s,w,a} \boldsymbol{b}_\alpha(\boldsymbol{x}) \cdot \Delta \boldsymbol{y}_\alpha(\boldsymbol{x}) \right\} \mathrm{d}V. \end{aligned} \tag{13}$$

Since $\boldsymbol{y}_s$, $\boldsymbol{y}_w$ and $\boldsymbol{y}_a$ can be varied independently, their respective first variations must vanish. From the $\boldsymbol{y}_s$ variation,

$$\begin{aligned} 0 = & \int_{\mathcal{B}} \left\{ \int_{\mathcal{H}} \left[\underline{\boldsymbol{T}}_{ss}[\boldsymbol{x}]\langle \boldsymbol{x}' - \boldsymbol{x}\rangle \cdot \Delta \boldsymbol{y}_s(\boldsymbol{x}') - \underline{\boldsymbol{T}}_{ss}[\boldsymbol{x}]\langle \boldsymbol{x}' - \boldsymbol{x}\rangle \cdot \Delta \boldsymbol{y}_s(\boldsymbol{x}) \right. \right. \\ & \left. \left. + \sum_{\alpha=w,a} \left(\underline{\boldsymbol{T}}_{s\alpha}[\boldsymbol{x}]\langle \boldsymbol{x}' - \boldsymbol{x}\rangle \cdot \Delta \boldsymbol{y}_s(\boldsymbol{x}') - \underline{\boldsymbol{T}}_{\alpha s}[\boldsymbol{x}]\langle \boldsymbol{x}' - \boldsymbol{x}\rangle \cdot \Delta \boldsymbol{y}_s(\boldsymbol{x}) \right) \right] \mathrm{d}V' - \boldsymbol{b}_s(\boldsymbol{x}) \cdot \Delta \boldsymbol{y}_s(\boldsymbol{x}) \right\} \mathrm{d}V. \end{aligned} \tag{14}$$

Interchanging the dummy variables of integration $\boldsymbol{x} \leftrightarrow \boldsymbol{x}'$ in the first and third terms in the integrand leads to

$$\begin{aligned} 0 = & \int_{\mathcal{B}} \left\{ \int_{\mathcal{H}} \left[\underline{\boldsymbol{T}}_{ss}[\boldsymbol{x}']\langle \boldsymbol{x} - \boldsymbol{x}'\rangle \cdot \Delta \boldsymbol{y}_s(\boldsymbol{x}) - \underline{\boldsymbol{T}}_{ss}[\boldsymbol{x}]\langle \boldsymbol{x}' - \boldsymbol{x}\rangle \cdot \Delta \boldsymbol{y}_s(\boldsymbol{x}) \right. \right. \\ & \left. \left. + \sum_{\alpha=w,a} \left(\underline{\boldsymbol{T}}_{s\alpha}[\boldsymbol{x}']\langle \boldsymbol{x} - \boldsymbol{x}'\rangle \cdot \Delta \boldsymbol{y}_s(\boldsymbol{x}) - \underline{\boldsymbol{T}}_{\alpha s}[\boldsymbol{x}]\langle \boldsymbol{x}' - \boldsymbol{x}\rangle \cdot \Delta \boldsymbol{y}_s(\boldsymbol{x}) \right) \right] \mathrm{d}V' - \boldsymbol{b}_s(\boldsymbol{x}) \cdot \Delta \boldsymbol{y}_s(\boldsymbol{x}) \right\} \mathrm{d}V. \end{aligned} \tag{15}$$

Hence

$$0=\int_{\mathcal{B}}\left\{\int_{\mathcal{H}}\left[\underline{\mathbf{T}}_{ss}[\mathbf{x}']\langle\mathbf{x}-\mathbf{x}'\rangle-\underline{\mathbf{T}}_{ss}[\mathbf{x}]\langle\mathbf{x}'-\mathbf{x}\rangle+\sum_{\alpha=w,a}\left(\underline{\mathbf{T}}_{s\alpha}[\mathbf{x}']\langle\mathbf{x}-\mathbf{x}'\rangle-\underline{\mathbf{T}}_{\alpha s}[\mathbf{x}]\langle\mathbf{x}'-\mathbf{x}\rangle\right)\right]\mathrm{d}V'-\mathbf{b}_s(\mathbf{x})\right\}\cdot\Delta\mathbf{y}_s(\mathbf{x})\mathrm{d}V. \tag{16}$$

Since this must hold for every choice of $\Delta\boldsymbol{y}_s$, it follows that

$$0=\int_{\mathcal{H}}\left(\underline{\boldsymbol{T}}_{ss}[\boldsymbol{x}]\langle\boldsymbol{x}'-\boldsymbol{x}\rangle-\underline{\boldsymbol{T}}_{ss}[\boldsymbol{x}']\langle\boldsymbol{x}-\boldsymbol{x}'\rangle\right)\mathrm{d}V'+\int_{\mathcal{H}}\sum_{\alpha=w,a}\left(\underline{\boldsymbol{T}}_{\alpha s}[\boldsymbol{x}]\langle\boldsymbol{x}+\boldsymbol{x}\rangle-\underline{\boldsymbol{T}}_{s\alpha}[\boldsymbol{x}']\langle\boldsymbol{x}-\boldsymbol{x}'\rangle\right)\mathrm{d}V'+\boldsymbol{b}_s(\boldsymbol{x}) \tag{17}$$

for all $\boldsymbol{x}\in\mathcal{B}$. Similarly, for the fluid phases from the first variation with respect to $\Delta\boldsymbol{y}_\alpha$,

$$0=\int_{\mathcal{H}}\left(\underline{\boldsymbol{T}}_{\alpha\alpha}[\boldsymbol{x}]\langle\boldsymbol{x}'-\boldsymbol{x}\rangle-\underline{\boldsymbol{T}}_{\alpha\alpha}[\boldsymbol{x}']\langle\boldsymbol{x}-\boldsymbol{x}'\rangle\right)\mathrm{d}V'+\int_{\mathcal{H}}\left(\underline{\boldsymbol{T}}_{s\alpha}[\boldsymbol{x}]\langle\boldsymbol{x}+\boldsymbol{x}\rangle-\underline{\boldsymbol{T}}_{\alpha s}[\boldsymbol{x}']\langle\boldsymbol{x}-\boldsymbol{x}'\rangle\right)\mathrm{d}V'+\boldsymbol{b}_\alpha(\boldsymbol{x}) \tag{18}$$

for all $\boldsymbol{x}\in\mathcal{B}$, where $\alpha=w,a$.

Finally, the equations of motion for each phase for $\boldsymbol{x}\in\mathcal{B}$ are given by

$$\begin{aligned}\rho^s\ddot{\boldsymbol{y}}_s(\boldsymbol{x}) &= \int_{\mathcal{H}}\left(\underline{\boldsymbol{T}}_{ss}[\boldsymbol{x}]\langle\boldsymbol{x}'-\boldsymbol{x}\rangle-\underline{\boldsymbol{T}}_{ss}[\boldsymbol{x}']\langle\boldsymbol{x}-\boldsymbol{x}'\rangle\right)\mathrm{d}V'+\int_{\mathcal{H}}\left(\underline{\boldsymbol{T}}_{ws}[\boldsymbol{x}]\langle\boldsymbol{x}'-\boldsymbol{x}\rangle-\underline{\boldsymbol{T}}_{sw}[\boldsymbol{x}']\langle\boldsymbol{x}-\boldsymbol{x}'\rangle\right)\mathrm{d}V'\\ &\quad+\int_{\mathcal{H}}\left(\underline{\boldsymbol{T}}_{as}[\boldsymbol{x}]\langle\boldsymbol{x}'-\boldsymbol{x}\rangle-\underline{\boldsymbol{T}}_{sa}[\boldsymbol{x}']\langle\boldsymbol{x}-\boldsymbol{x}'\rangle\right)\mathrm{d}V'+\boldsymbol{b}_s(\boldsymbol{x}),\end{aligned} \tag{19}$$

$$\begin{aligned}\rho^w\ddot{\mathbf{y}}_w(\mathbf{x}) &= \int_{\mathcal{H}}\left(\underline{\mathbf{T}}_{ww}[\mathbf{x}]\langle\mathbf{x}'-\mathbf{x}\rangle-\underline{\mathbf{T}}_{ww}[\mathbf{x}']\langle\mathbf{x}-\mathbf{x}'\rangle\right)\mathrm{d}V'\\ &\quad+\int_{\mathcal{H}}\left(\underline{\mathbf{T}}_{sw}[\mathbf{x}]\langle\mathbf{x}'-\mathbf{x}\rangle-\underline{\mathbf{T}}_{ws}[\mathbf{x}']\langle\mathbf{x}-\mathbf{x}'\rangle\right)\mathrm{d}V'+\mathbf{b}_w(\mathbf{x}),\end{aligned} \tag{20}$$

$$\rho^a\ddot{\boldsymbol{y}}_a(\boldsymbol{x})=\int_{\mathcal{H}}\left(\underline{\boldsymbol{T}}_{aa}[\boldsymbol{x}]\langle\boldsymbol{x}'-\boldsymbol{x}\rangle-\underline{\boldsymbol{T}}_{aa}[\boldsymbol{x}']\langle\boldsymbol{x}-\boldsymbol{x}'\rangle\right)\mathrm{d}V'+\int_{\mathcal{H}}\left(\underline{\boldsymbol{T}}_{sa}[\boldsymbol{x}]\langle\boldsymbol{x}'-\boldsymbol{x}\rangle-\underline{\boldsymbol{T}}_{as}[\boldsymbol{x}']\langle\boldsymbol{x}-\boldsymbol{x}'\rangle\right)\mathrm{d}V'+\boldsymbol{b}_a(\boldsymbol{x}), \tag{21}$$

where $\ddot{\boldsymbol{y}}_s,\ddot{\boldsymbol{y}}_w$, and $\ddot{\boldsymbol{y}}_a$ are the accelerations of the solid skeleton, pore water and pore air, respectively. Summation of (19), (20), and (21) yields the motion of the three-phase porous mixture as follows,

$$\sum_{\alpha=s,w,a}\left(\rho^\alpha\ddot{\boldsymbol{y}}_\alpha\right)=\int_{\mathcal{H}}\left(\underline{\boldsymbol{T}}[\boldsymbol{x}]\langle\boldsymbol{x}'-\boldsymbol{x}\rangle-\underline{\boldsymbol{T}}[\boldsymbol{x}']\langle\boldsymbol{x}-\boldsymbol{x}'\rangle\right)\mathrm{d}V'+\sum_{\alpha=s,w,a}\boldsymbol{b}_\alpha(\boldsymbol{x}), \tag{22}$$

where

$$\underline{\boldsymbol{T}}[\boldsymbol{x}]\langle\boldsymbol{x}'-\boldsymbol{x}\rangle=\sum_{\alpha=s,w,a}\underline{\boldsymbol{T}}_{\alpha\alpha}[\boldsymbol{x}]\langle\boldsymbol{x}'-\boldsymbol{x}\rangle, \tag{23}$$

$$\underline{\boldsymbol{T}}[\boldsymbol{x}']\langle\boldsymbol{x}-\boldsymbol{x}'\rangle=\sum_{\alpha=s,w,a}\underline{\boldsymbol{T}}_{\alpha\alpha}[\boldsymbol{x}']\langle\boldsymbol{x}-\boldsymbol{x}'\rangle. \tag{24}$$

Let $\tilde{\boldsymbol{a}}_\alpha=\boldsymbol{a}_\alpha-\boldsymbol{a}_s$ be the relative material acceleration of fluid α to that of the solid phase, we have

$$\int_{\mathcal{H}}\left(\underline{\boldsymbol{T}}[\boldsymbol{x}]\langle\boldsymbol{x}'-\boldsymbol{x}\rangle-\underline{\boldsymbol{T}}[\boldsymbol{x}']\langle\boldsymbol{x}-\boldsymbol{x}'\rangle\right)\mathrm{d}V'+\rho(\boldsymbol{g}-\boldsymbol{a})-\sum_{\alpha=\mathrm{w,a}}\rho^\alpha\tilde{\boldsymbol{a}}_\alpha=\boldsymbol{0}. \tag{25}$$

For conciseness, Eq. (25) can be written as

$$\int_{\mathcal{H}}\left(\underline{\boldsymbol{T}}-\underline{\boldsymbol{T}}'\right)\mathrm{d}V'+\rho(\boldsymbol{g}-\boldsymbol{a})-\sum_{\alpha=\mathrm{w,a}}\rho^\alpha\tilde{\boldsymbol{a}}_\alpha=\boldsymbol{0}, \tag{26}$$

where $\underline{\boldsymbol{T}}$ is the total force state along $\boldsymbol{x}'-\boldsymbol{x}$ at $\boldsymbol{x}$ and $\underline{\boldsymbol{T}}'$ is the total force state along $\boldsymbol{x}-\boldsymbol{x}'$ at $\boldsymbol{x}'$. The same notation is adopted for conciseness in the remaining article.

2.3. Balance of mass of unsaturated porous media

To formulate the balance of mass of unsaturated porous media, we first introduce the bond extension states. The bond extension states for the solid phase and the fluid phases are given by

$$\underline{e}_{ss}\langle\boldsymbol{\xi}\rangle=|\underline{\boldsymbol{Y}}_{ss}|-|\boldsymbol{\xi}|, \tag{27}$$

$$\underline{e}_{ww}\langle\boldsymbol{\xi}\rangle=|\underline{\boldsymbol{Y}}_{ww}|-|\boldsymbol{\xi}|, \tag{28}$$

$$\underline{e}_{\alpha\alpha}\langle\boldsymbol{\xi}\rangle = |\underline{\boldsymbol{Y}}_{\alpha\alpha}| - |\boldsymbol{\xi}|, \tag{29}$$

where $\boldsymbol{\xi} = \boldsymbol{x}' - \boldsymbol{x}$. For the small deformation, the rate form of the bond extension states can be approximated as

$$\dot{\underline{e}}_{\alpha\alpha} = \left|\dot{\underline{\boldsymbol{Y}}}_{\alpha\alpha}\langle\boldsymbol{\xi}\rangle\right| = \dot{\underline{\boldsymbol{U}}}_{\alpha\alpha} \cdot \underline{\boldsymbol{M}}\langle\boldsymbol{\xi}\rangle = \dot{\underline{\boldsymbol{Y}}}_{\alpha\alpha} \cdot \underline{\boldsymbol{M}}\langle\boldsymbol{\xi}\rangle, \quad \text{with} \quad \alpha = s, w, a, \tag{30}$$

where $\underline{\boldsymbol{U}}_{\alpha\alpha}$ is the displacement state defined by

$$\underline{\boldsymbol{U}}_{\alpha\alpha}\langle\boldsymbol{\xi}\rangle = \underline{\boldsymbol{Y}}_{\alpha\alpha}\langle\boldsymbol{\xi}\rangle - \boldsymbol{\xi}, \tag{31}$$

and $\underline{\boldsymbol{M}}$ is the bond direction defined by

$$\underline{\boldsymbol{M}}\langle\boldsymbol{\xi}\rangle = \frac{\boldsymbol{\xi}}{|\boldsymbol{\xi}|}. \tag{32}$$

The rate form of the nonlocal dilation state for the phase α is defined by

$$\dot{\underline{\vartheta}}_{\alpha\alpha} = \frac{3\left(\underline{\omega}\,\underline{x}\right) \bullet \dot{\underline{e}}_{\alpha\alpha}}{m}, \tag{33}$$

where $\underline{\omega}$ is a non-negative scalar function, called influence function. Influence function is a non-negative scalar state defined on $\mathcal{H}$ (Silling et al., 2007). The influence function plays the role in weighting the contribution of all the bonds participating in the computation of volume-dependent properties.

The scalar state $\underline{x}$ is defined by

$$\underline{x}\langle\boldsymbol{\xi}\rangle = |\boldsymbol{\xi}| \tag{34}$$

for any bond $\boldsymbol{\xi}$, and m is the weighted volume defined by

$$m = \left(\underline{\omega}\,\underline{x}\right) \bullet \underline{x}. \tag{35}$$

Substituting Eq. (30) into Eq. (33) yields the rate form of dilation or volume change in terms of the rate of deformation state of each phase as

$$\dot{\underline{\vartheta}}_{\alpha\alpha} = \frac{3\left(\underline{\omega}\,\underline{x}\right) \bullet \dot{\underline{\boldsymbol{Y}}}_{\alpha\alpha}}{m} \cdot \underline{\boldsymbol{M}}\langle\boldsymbol{\xi}\rangle, \quad \text{with} \quad \alpha = s, w, a. \tag{36}$$

Referring to the mass balance equation of classic unsaturated poromechanics (see Appendix B), the mass balance equation for each phase of the mixture in peridynamics can be cast as follows. The mass balance of the solid skeleton reads

$$\frac{\mathrm{d}\phi^s}{\mathrm{d}t} + \frac{\phi^s}{K_s}\frac{\mathrm{d}p_s}{\mathrm{d}t} + \phi^s \int_{\mathcal{H}} \frac{3\left(\underline{\omega}\,\underline{x}\right)\dot{\underline{\boldsymbol{Y}}}_{ss}}{m} \cdot \underline{\boldsymbol{M}}\langle\boldsymbol{\xi}\rangle \mathrm{d}V' = 0, \tag{37}$$

where ϕ^s, K_s and p_s are the volume fraction, the bulk modulus, and the mean pressure of the solid phase respectively as introduced in Appendix B. The mass balance of pore water reads,

$$(1-\phi^s)\frac{\mathrm{d}\psi^w}{\mathrm{d}t} + \frac{\phi^w}{K_w}\frac{\mathrm{d}p_w}{\mathrm{d}t} + \psi^w B \int_{\mathcal{H}} \left(\frac{3\left(\underline{\omega}\,\underline{x}\right)\dot{\underline{\boldsymbol{Y}}}_{ss}}{m} \cdot \underline{\boldsymbol{M}}\langle\boldsymbol{\xi}\rangle \right) \mathrm{d}V' + \frac{1}{\rho_w}\int_{\mathcal{H}} \left(\phi^w \rho_w \frac{3\left(\underline{\omega}\,\underline{x}\right)\dot{\underline{\boldsymbol{Y}}}_{ww}}{m} \cdot \underline{\boldsymbol{M}}\langle\boldsymbol{\xi}\rangle \right) \mathrm{d}V' = 0, \tag{38}$$

where ψ^w is the degree of saturation of water, K_w is the bulk modulus of water, p_w is water pressure, and ϕ^w is the volume fraction of water, B is a coefficient as defined in Appendix B, $\dot{\underline{\boldsymbol{Y}}}_{ww}$ is the rate of relative flow state of pore water at point $\boldsymbol{x}'$ on the bond $\langle \boldsymbol{x}' - \boldsymbol{x}\rangle$ defined by

$$\dot{\underline{\boldsymbol{Y}}}_{ww} = \dot{\underline{\boldsymbol{Y}}}_{ww} - \dot{\underline{\boldsymbol{Y}}}_{ss}. \tag{39}$$

Similarly, the mass balance of pore air reads,

$$(1-\phi^s)\frac{\mathrm{d}\psi^a}{\mathrm{d}t}+\frac{\phi^a}{K_a}\frac{\mathrm{d}p_a}{\mathrm{d}t}+\psi^a B\int_{\mathcal{H}}\left(\frac{3\left(\underline{\omega}\,\underline{x}\right)\dot{\underline{Y}}_{ss}}{m}\cdot\underline{\boldsymbol{M}}\langle\boldsymbol{\xi}\rangle\right)\mathrm{d}V'+\frac{1}{\rho_a}\int_{\mathcal{H}}\left(\phi^a\rho_a\frac{3\left(\underline{\omega}\,\underline{x}\right)\dot{\underline{\dot{Y}}}_{aa}}{m}\cdot\underline{\boldsymbol{M}}\langle\boldsymbol{\xi}\rangle\right)\mathrm{d}V'=0, \tag{40}$$

where ψ^a is the degree of saturation of air, ϕ^a is the volume fraction of air, K_a is the bulk modulus of air, p_a is air pressure, $\dot{\underline{\dot{Y}}}_{aa}$ is the rate of relative flow state of pore air at point $\boldsymbol{x}'$ on the bond $\langle\boldsymbol{x}'-\boldsymbol{x}\rangle$ defined by

$$\dot{\underline{\dot{Y}}}_{aa}=\dot{\underline{Y}}_{aa}-\dot{\underline{Y}}_{ss}. \tag{41}$$

It is noted that both peridynamic balance equations of water and air account for the mass change of water and air induced by the deformation of the solid skeleton. Recall $\dot{\boldsymbol{Y}}_{ss}=\dot{\boldsymbol{y}}_s'-\dot{\boldsymbol{y}}_s$ and $\dot{\underline{\dot{Y}}}_{a\alpha}=\dot{\underline{Y}}_{a\alpha}-\dot{\underline{Y}}_{ss}$ with $\alpha=w,a$. Thus, the peridynamic mass balance equations can be written as

$$(1-\phi^s)\frac{\mathrm{d}\psi^\alpha}{\mathrm{d}t}+\frac{\phi^\alpha}{K_\alpha}\frac{\mathrm{d}p_\alpha}{\mathrm{d}t}+\psi^\alpha B\int_{\mathcal{H}}\left(\frac{3\left(\underline{\omega}\,\underline{x}\right)}{m}\underline{\mathbf{M}}\langle\boldsymbol{\xi}\rangle\cdot\left(\dot{\mathbf{y}}_s'-\dot{\mathbf{y}}_s\right)\right)\mathrm{d}V'+\frac{1}{\rho_\alpha}\int_{\mathcal{H}}\left(\phi^\alpha\rho_\alpha\frac{3\left(\underline{\omega}\,\underline{x}\right)}{m}\underline{\mathbf{M}}\langle\boldsymbol{\xi}\rangle\cdot\left(\dot{\tilde{\mathbf{y}}}_\alpha'-\dot{\tilde{\mathbf{y}}}_\alpha\right)\right)\mathrm{d}V'=0, \tag{42}$$

where $\dot{\tilde{\boldsymbol{y}}}_\alpha'=\dot{\boldsymbol{y}}_\alpha'-\dot{\boldsymbol{y}}_s'$ and $\dot{\tilde{\boldsymbol{y}}}_\alpha=\dot{\boldsymbol{y}}_\alpha-\dot{\boldsymbol{y}}_s$. The Eq. (42) can be named by the ordinary state-based peridynamic mass balance equations in the sense that the mass or volume flux can only occur along the bond directions. This is similar to the definition in the peridynamic solid mechanics (Silling et al., 2007).

Furthermore, a generalized state-based peridynamic balance of mass for fluid phases may be formulated by postulating the mass flow state of fluids as follows. Let $\underline{Q}_\alpha$ and $\underline{Q}_\alpha'$ with $\alpha=w,a$ be the mass flow state of the α phase with respect to the solid skeleton at points $\boldsymbol{x}$ and $\boldsymbol{x}'$, respectively. The peridynamic mass balance equation of the two pore fluid phases can be written as

$$(1-\phi^s)\frac{\mathrm{d}\psi^\alpha}{\mathrm{d}t}+\frac{\phi^\alpha}{K_\alpha}\frac{\mathrm{d}p_\alpha}{\mathrm{d}t}+\psi^\alpha B\int_{\mathcal{H}}\left(\underline{Q}_s'-\underline{Q}_s\right)\mathrm{d}V'+\frac{1}{\rho_\alpha}\int_{\mathcal{H}}\left(\tilde{\underline{Q}}_\alpha'-\tilde{\underline{Q}}_\alpha\right)\mathrm{d}V'=0, \tag{43}$$

where $\underline{Q}_s$ and $\underline{Q}_s'$ are the rate of volume change of the solid skeleton at points $\boldsymbol{x}$ and $\boldsymbol{x}'$, respectively. In Section 4.3, we will provide the mathematical forms for $\underline{Q}_\alpha$ and $\underline{Q}_\alpha'$ with $\alpha=w,a$, and $\underline{Q}_s$ and $\underline{Q}_s'$ for peridynamic unsaturated porous materials through the multiphase constitutive correspondence principle.

In the peridynamics theory, the requirement of boundary conditions does not mathematically emerge because the peridynamic field equations do not contain any spatial derivatives (Silling, 2000). Volumetric constraints instead of surface constraints in an equivalent boundary value problems are usually utilized in the nonlocal peridynamic formulation. These volume constraints can be imposed in a nonlocal region along the boundary, constraining the solution in a nonzero volume. The *essential boundary condition* (i.e., displacement or pore fluid pressure) can be imposed by assigning constraints to the material points in the fictitious boundary layer. The *natural boundary condition* (i.e., flux type) can be enforced by approximating the value of the potential in the fictitious region so that the variation of the potential both in the real problem domain and the fictitious boundary layer recovers the applied flux value on the surface. For the case of zero flux, it can be satisfied naturally without prescribing any specific constraint.

3. Effective force state and thermodynamcs restrictions on constitutive models

The peridynamics governing equations for unsaturated porous media formulated in the previous section is general in the sense that no material models (e.g., effective force state and deformation state) are incorporated. This section deals with the effective force state for the solid skeleton and thermodynamic restrictions on the constitutive models for unsaturated peri-poromechanics. The effective force state of the unsaturated porous medium is a peridynamic constitutive force state through which unsaturated porous media can be treated as an equivalent single-phase and single-force state peridynamic material. By applying the balance of energy of the three-phase porous media, the effective force state is derived as an energy conjugate of the nonlocal deformation state of the solid skeleton, and the suction force state is defined as the difference between pore air force state and pore water force state. By applying entropy inequality of unsaturated porous media the thermodyanmics restriction on constitutive models and physical laws are presented for unsaturated peri-poromechanics.

3.1. Effective force state of unsaturated porous media

In this part, the effective force state of the three-phase porous media will be derived through the energy balance. The energy balance involves both mechanical power and non-mechanical power (e.g., heat transport) of the porous media. Our objective is to formulate a work conjugate expression for the constitutive modeling of the poromechanical behavior of unsaturated porous media. Thus, for brevity we shall focus on the mechanical power in what follows and ignore the heat transport. The global energy balance introduces both the *absorbed power* and *supplied power* for a part of the three-phase material body. In this way, the internal energy defined in terms of these powers is an additive quantity, leading to a meaningful definition of internal energy, which is different from

the conventional nonlocal theory (Silling and Lehoucq, 2010). For brevity, we omit the content in the square bracket and angle bracket in the following derivation. For the solid phase, taking the scalar product of both sides of the balance of linear momentum of the solid phase (Eq. (19)) with the velocity $\boldsymbol{v}_s$ and integrating over $\mathcal{P}$ yields

$$\begin{aligned}\frac{\mathrm{d}}{\mathrm{d}t}\int_{\mathcal{P}}\frac{\rho^s\mathbf{v}_s\cdot\mathbf{v}_s}{2}\mathrm{d}V &= \int_{\mathcal{P}}\int_{\mathcal{H}}\left(\underline{\mathbf{T}}_{ss}-\underline{\mathbf{T}}'_{ss}\right)\cdot\mathbf{v}_s\mathrm{d}V'\mathrm{d}V+\int_{\mathcal{P}}\int_{\mathcal{H}}\left(\underline{\mathbf{T}}_{ws}-\underline{\mathbf{T}}'_{sw}\right)\cdot\mathbf{v}_s\mathrm{d}V'\mathrm{d}V\\ &+\int_{\mathcal{P}}\int_{\mathcal{H}}\left(\underline{\mathbf{T}}_{as}-\underline{\mathbf{T}}'_{sa}\right)\cdot\mathbf{v}_s\mathrm{d}V'\mathrm{d}V+\int_{\mathcal{P}}\mathbf{b}_s\cdot\mathbf{v}_s\mathrm{d}V.\end{aligned}\tag{44}$$

Note that $\boldsymbol{T}_{ss}$, $\boldsymbol{T}_{ws}$ and $\boldsymbol{T}_{as}=0$ whenever $\boldsymbol{x}'\notin\mathcal{H}$ (i.e., the point $\boldsymbol{x}$ only has mechanical interactions with points in its family). It follows from Eq. (44) that

$$\begin{aligned}\frac{\mathrm{d}}{\mathrm{d}t}\int_{\mathcal{P}}\frac{\rho^s\mathbf{v}_s\cdot\mathbf{v}_s}{2}\mathrm{d}V &= \int_{\mathcal{P}}\int_{\mathcal{B}}\left(\underline{\mathbf{T}}_{ss}-\underline{\mathbf{T}}'_{ss}\right)\cdot\mathbf{v}_s\mathrm{d}V'\mathrm{d}V+\int_{\mathcal{P}}\int_{\mathcal{B}}\left(\underline{\mathbf{T}}_{ws}-\underline{\mathbf{T}}'_{sw}\right)\cdot\mathbf{v}_s\mathrm{d}V'\mathrm{d}V\\ &+\int_{\mathcal{P}}\int_{\mathcal{B}}\left(\underline{\mathbf{T}}_{as}-\underline{\mathbf{T}}'_{sa}\right)\cdot\mathbf{v}_s\mathrm{d}V'\mathrm{d}V+\int_{\mathcal{P}}\mathbf{b}_s\cdot\mathbf{v}_s\mathrm{d}V.\end{aligned}\tag{45}$$

With the identity

$$\begin{aligned}&\int_{\mathcal{P}}\int_{\mathcal{B}}\left(\underline{\mathbf{T}}_{ss}-\underline{\mathbf{T}}'_{ss}\right)\cdot\mathbf{v}_s\mathrm{d}V'\mathrm{d}V=\int_{\mathcal{P}}\int_{\mathcal{B}}\left(\underline{\mathbf{T}}_{ss}\cdot\mathbf{v}'_s-\underline{\mathbf{T}}'_{ss}\cdot\mathbf{v}_s\right)\mathrm{d}V'\mathrm{d}V\\ -\int_{\mathcal{P}}\int_{\mathcal{B}}\underline{\mathbf{T}}_{ss}\cdot\left(\mathbf{v}'_s-\mathbf{v}_s\right)\mathrm{d}V'\mathrm{d}V &= \int_{\mathcal{P}}\int_{\mathcal{B}\setminus\mathcal{P}}\left(\underline{\mathbf{T}}_{ss}\cdot\mathbf{v}'_s-\underline{\mathbf{T}}'_{ss}\cdot\mathbf{v}_s\right)\mathrm{d}V'\mathrm{d}V-\int_{\mathcal{P}}\int_{\mathcal{B}}\underline{\mathbf{T}}_{ss}\cdot\left(\mathbf{v}'_s-\mathbf{v}_s\right)\mathrm{d}V'\mathrm{d}V,\end{aligned}\tag{47}$$

$$\left(\underline{\boldsymbol{T}}_{ss}-\underline{\boldsymbol{T}}'_{ss}\right)\cdot\boldsymbol{v}_s=\left(\underline{\boldsymbol{T}}_{ss}\cdot\boldsymbol{v}'_s-\underline{\boldsymbol{T}}'_{ss}\cdot\boldsymbol{v}_s\right)-\underline{\boldsymbol{T}}_{ss}\cdot\left(\boldsymbol{v}'_s-\boldsymbol{v}_s\right),\tag{46}$$

the first term on the right-hand side of Eq. (44) can be written as for all $\mathcal{P}\subset\mathcal{B}$,

where the anti-symmetry of the *dual power density*

$$p^s_d(\boldsymbol{x}',\boldsymbol{x})=\underline{\boldsymbol{T}}_{ss}\cdot\boldsymbol{v}'_s-\underline{\boldsymbol{T}}'_{ss}\cdot\boldsymbol{v}_s\tag{48}$$

is used in the last step. Applying the same operations to the second and third terms on the right-hand side of Eq. (44) (i.e., the interaction force states between the solid and the fluids), the power *absorbed* by the solid skeleton of $\mathcal{P}$ can be defined as

$$\mathcal{W}^s_{\mathrm{abs}}(\mathcal{P})=\int_{\mathcal{P}}\int_{\mathcal{B}}\underline{\boldsymbol{T}}_{ss}\cdot\left(\boldsymbol{v}'_s-\boldsymbol{v}_s\right)\mathrm{d}V'\mathrm{d}V.\tag{49}$$

The power supplied to the solid skeleton of $\mathcal{P}$ can be defined as

$$\mathcal{W}^s_{\mathrm{sup}} = \int_{\mathcal{P}}\int_{\mathcal{B}\setminus\mathcal{P}}\left(\left(\underline{\mathbf{T}}_{ss}+\underline{\mathbf{T}}_{ws}+\underline{\mathbf{T}}_{as}\right)\cdot\mathbf{v}'_s-\left(\underline{\mathbf{T}}'_{ss}+\underline{\mathbf{T}}'_{ws}+\underline{\mathbf{T}}'_{as}\right)\cdot\mathbf{v}_s\right)\mathrm{d}V'\mathrm{d}V+\int_{\mathcal{P}}\int_{\mathcal{B}}\left(\underline{\mathbf{T}}_{ws}+\underline{\mathbf{T}}_{as}\right)\cdot\left(\mathbf{v}'_s-\mathbf{v}_s\right)\mathrm{d}V'\mathrm{d}V+\int_{\mathcal{P}}\mathbf{b}_s\cdot\mathbf{v}_s\mathrm{d}V.\tag{50}$$

Multiply Eqs. (20) and (21) by $\boldsymbol{v}_w$ and $\boldsymbol{v}_a$ respectively and integrate over $\mathcal{P}$. Following the same operations on Eq. (45), the power *absorbed* by the pore fluids in $\mathcal{P}$ can be written as

$$\mathcal{W}^w_{\mathrm{abs}}(\mathcal{P})=\int_{\mathcal{P}}\int_{\mathcal{B}}\underline{\boldsymbol{T}}_{ww}\cdot\left(\boldsymbol{v}'_w-\boldsymbol{v}_w\right)\mathrm{d}V'\mathrm{d}V,\tag{51}$$

$$\mathcal{W}^a_{\mathrm{abs}}(\mathcal{P})=\int_{\mathcal{P}}\int_{\mathcal{B}}\underline{\boldsymbol{T}}_{aa}\cdot\left(\boldsymbol{v}'_a-\boldsymbol{v}_a\right)\mathrm{d}V'\mathrm{d}V,\tag{52}$$

where $\boldsymbol{v}_\alpha$ and $\boldsymbol{v}'_\alpha$ with $\alpha=w,a$ are the velocity of pore fluids at $\boldsymbol{x}$ and $\boldsymbol{x}'$, respectively. The power *supplied* to the pore fluids in $\mathcal{P}$ can be written as

$$\mathcal{W}^w_{\mathrm{sup}} = \int_{\mathcal{P}}\int_{\mathcal{B}\setminus\mathcal{P}}\left(\left(\underline{\mathbf{T}}_{ww}+\underline{\mathbf{T}}_{sw}\right)\cdot\mathbf{v}'_w-\left(\underline{\mathbf{T}}'_{ww}+\underline{\mathbf{T}}'_{sw}\right)\cdot\mathbf{v}_w\right)\mathrm{d}V'\mathrm{d}V+\int_{\mathcal{P}}\int_{\mathcal{B}}\underline{\mathbf{T}}_{sw}\cdot\left(\mathbf{v}'_w-\mathbf{v}_w\right)\mathrm{d}V'\mathrm{d}V+\int_{\mathcal{P}}\mathbf{b}_w\cdot\mathbf{v}_w\mathrm{d}V,\tag{53}$$

$$\mathcal{W}_{\text{sup}}^{a} = \int_{\mathcal{P}}\int_{\mathcal{B}\setminus\mathcal{P}} \Big(\Big(\underline{\boldsymbol{T}}_{aa} + \underline{\boldsymbol{T}}_{sa} \Big) \cdot \boldsymbol{v}_a^{'} - \Big(\underline{\boldsymbol{T}}_{aa}^{'} + \underline{\boldsymbol{T}}_{sa}^{'} \Big) \cdot \boldsymbol{v}_a \Big) \mathrm{d}V^{'} \mathrm{d}V + \int_{\mathcal{P}}\int_{\mathcal{B}} \underline{\boldsymbol{T}}_{sa} \cdot \big(\boldsymbol{v}_a^{'} - \boldsymbol{v}_a \big) \mathrm{d}V^{'} \mathrm{d}V + \int_{\mathcal{P}} \boldsymbol{b}_a \cdot \boldsymbol{v}_a \mathrm{d}V. \tag{54}$$

Next, we define the kinetic energy of the solid and fluid phases in $\mathcal{P}$ as

$$\mathcal{K}^{\alpha}(\mathcal{P}) = \int_{\mathcal{P}} \frac{\rho^{\alpha} \boldsymbol{v}_{\alpha} \cdot \boldsymbol{v}_{\alpha}}{2} \mathrm{d}V \quad \text{with} \quad \alpha = s, w, a. \tag{55}$$

Now we can express the power balance of the three-phase porous material as

$$\dot{\mathcal{K}}(\mathcal{P}) + \mathcal{W}_{\text{abs}}(\mathcal{P}) = \mathcal{W}_{\text{sub}}, \tag{56}$$

where

$$\dot{\mathcal{K}}(\mathcal{P}) = \sum_{\alpha=s,w,a} \dot{\mathcal{K}}^{\alpha}(\mathcal{P}), \tag{57}$$

$$\mathcal{W}_{\text{abs}}(\mathcal{P}) = \sum_{\alpha=s,w,a} \mathcal{W}_{\text{abs}}^{\alpha}(\mathcal{P}), \tag{58}$$

$$\mathcal{W}_{\text{sub}} = \sum_{\alpha=s,w,a} \mathcal{W}_{\text{sub}}^{\alpha}(\mathcal{P}). \tag{59}$$

Here, we focus on deriving the effective force state of the solid skeleton in the framework of peridynamics. Without loss of generality, the isothermal condition is assumed for the three-phase porous material. In line with this assumption, we postulate the following global form of the energy balance (i.e., the first law of the thermodynamics) for the three-phase porous media:

$$\dot{\mathcal{E}} + \dot{\mathcal{K}} = \mathcal{W}_{\text{sup}}(\mathcal{P}), \tag{60}$$

where $\mathcal{E}(\mathcal{P})$ is the *internal energy* of the solid and fluids in $\mathcal{P}$. Subtracting (56) from (60) yields

$$\dot{\mathcal{E}}(\mathcal{P}) = \mathcal{W}_{\text{abs}}(\mathcal{P}), \tag{61}$$

in which the rate change of internal energy is the sum of the absorbed power. Let $\varepsilon(\boldsymbol{x}, t)$ be the *internal energy density* such that

$$\mathcal{E}(\mathcal{P}) = \int_{\mathcal{P}} \varepsilon \mathrm{d}V. \tag{62}$$

Summation of Eqs. (49), (51), and (52) generates

$$\int_{\mathcal{P}} \dot{\varepsilon} \mathrm{d}V = \int_{\mathcal{P}}\int_{\mathcal{B}} \sum_{\alpha=s,w,a} \underline{\boldsymbol{T}}_{a\alpha} \cdot \big(\boldsymbol{v}_{\alpha}^{'} - \boldsymbol{v}_{\alpha} \big) \mathrm{d}V^{'} \mathrm{d}V. \tag{63}$$

Since this must hold for any $\mathcal{P} \subset \mathcal{B}$, localization leads to the local statement of the first law of thermodynamics for three-phase porous media as follows,

$$\dot{\varepsilon} = p_{\text{abs}}, \tag{64}$$

where the absorbed power density at $\boldsymbol{x}$ is defined by

$$p_{\text{abs}} = \int_{\mathcal{B}} \sum_{\alpha=s,w,a} \underline{\boldsymbol{T}}_{a\alpha} \cdot \big(\boldsymbol{v}_{\alpha}^{'} - \boldsymbol{v}_{\alpha} \big) \mathrm{d}V^{'}. \tag{65}$$

By adding the null expression

$$\int_{\mathcal{B}} \Big(\underline{\boldsymbol{T}} - \underline{\boldsymbol{T}}_{ss} - \underline{\boldsymbol{T}}_{ww} - \underline{\boldsymbol{T}}_{aa} \Big) \cdot \big(\boldsymbol{v}_s^{'} - \boldsymbol{v}_s \big) \mathrm{d}V^{'} = 0 \tag{66}$$

into Eq. (65), we have

$$p_{\text{abs}} = \int_{\mathcal{B}} \underline{\mathbf{T}} \cdot \big(\mathbf{v}_s^{'} - \mathbf{v}_s \big) \mathrm{d}V^{'} + \int_{\mathcal{B}} \underline{\mathbf{T}}_{ww} \cdot \Big(\widetilde{\mathbf{v}}_w^{'} - \widetilde{\mathbf{v}}_w \Big) \mathrm{d}V^{'} + \int_{\mathcal{B}} \underline{\mathbf{T}}_{aa} \cdot \Big(\widetilde{\mathbf{v}}_a^{'} - \widetilde{\mathbf{v}}_a \Big) \mathrm{d}V^{'} = \int_{\mathcal{B}} \underline{\mathbf{T}} \cdot \underline{\dot{\mathbf{Y}}}_{ss} \mathrm{d}V^{'} + \int_{\mathcal{B}} \underline{\mathbf{T}}_{ww} \cdot \underline{\dot{\widetilde{\mathbf{Y}}}}_{ww} \mathrm{d}V^{'} + \int_{\mathcal{B}} \underline{\mathbf{T}}_{aa} \cdot \underline{\dot{\widetilde{\mathbf{Y}}}}_{aa} \mathrm{d}V^{'}. \tag{67}$$

To characterize the force state of fluids in unsaturated porous media, we define the force state for the fluid phase in terms of 'partial' fluid pressures (i.e., $\phi^{\alpha} p_{\alpha}$) as

$$\underline{\boldsymbol{T}}_{\alpha\alpha} = -\phi^{\alpha} p_{\alpha} 3\underline{\omega}\, \frac{\underline{x}\underline{\boldsymbol{M}}}{m}, \quad \alpha = w, a, \tag{68}$$

where ϕ^{α} and p_{α} are the volume fraction and intrinsic pore fluid pressure of the α fluid phase respectively as defined before. Substituting (68) into (67), we can express the absorbed power as

$$p_{\text{abs}} = \int_{\mathcal{B}} \underline{\boldsymbol{T}} \cdot \underline{\dot{\boldsymbol{Y}}}_{ss} \mathrm{d}V' - \int_{\mathcal{B}} \phi^{w} p_{w} \frac{3\underline{\omega}\, \underline{x}\underline{\boldsymbol{M}}}{m} \cdot \underline{\dot{\boldsymbol{Y}}}_{ww} \mathrm{d}V' - \int_{\mathcal{B}} \phi^{a} p_{a} \frac{3\underline{\omega}\, \underline{x}\underline{\boldsymbol{M}}}{m} \cdot \underline{\dot{\boldsymbol{Y}}}_{aa} \mathrm{d}V'. \tag{69}$$

Moreover, through Eq. (33), the absorbed power can be rewritten as

$$p_{\text{abs}} = \int_{\mathcal{B}} \underline{\boldsymbol{T}} \cdot \underline{\dot{\boldsymbol{Y}}}_{ss} \mathrm{d}V' - \int_{\mathcal{B}} \phi^{w} p_{w} \underline{\dot{\vartheta}}_{ww} \mathrm{d}V' - \int_{\mathcal{B}} \phi^{a} p_{a} \underline{\dot{\vartheta}}_{aa} \mathrm{d}V', \tag{70}$$

where $\underline{\dot{\vartheta}}_{\alpha\alpha}$ with $\alpha = w, a$ is the relative volume flow state of the α fluid phase with respect to the solid phase. Eqs. (69) and (70) demonstrate that the mechanical power of the partial force states is equal to the mechanical power of the total force state in deforming the solid skeleton plus the mechanical power of the pore fluid pressures in either injecting or extracting fluids into or from the solid matrix.

Next, multiply Eqs. (38) and (40) by p_w and p_a respectively and add them to the right-hand side of Eq. (70). By regrouping terms and applying Eq. (68), we have

$$p_{\text{abs}} = \left[\underline{\boldsymbol{T}} - B\left(\psi^{w}\underline{\boldsymbol{T}}_{w} + \psi^{a}\underline{\boldsymbol{T}}_{a}\right)\right] \bullet \underline{\dot{\boldsymbol{Y}}}_{ss} + \sum_{\alpha=w,a} (1-\phi^{s}) \frac{\mathrm{d}\psi^{\alpha}}{\mathrm{d}t} p_{\alpha} + \sum_{\alpha=w,a} \left[\frac{1}{\rho_{\alpha}} \left(\rho_{\alpha}\phi^{\alpha} \bullet \underline{\dot{\vartheta}}_{\alpha\alpha}\right) - \left(\phi^{\alpha} \bullet \underline{\dot{\vartheta}}_{\alpha\alpha}\right)\right] p_{\alpha} + \sum_{\alpha=w,a} \frac{\phi^{\alpha}}{K_{\alpha}} \frac{\mathrm{d}p_{\alpha}}{\mathrm{d}t} p_{\alpha}, \tag{71}$$

where $\underline{\boldsymbol{T}}_{\alpha}$ is the'intrinsic' force state of the α fluid phase which is written as

$$\underline{\boldsymbol{T}}_{\alpha} = -p_{\alpha} 3\underline{\omega}\, \frac{\underline{x}\underline{\boldsymbol{M}}}{m}, \quad \alpha = w, a. \tag{72}$$

The interpretation of Eq. (71) is as follows. The first term demonstrates that the quantity which is an energy conjugate to the rate of the deformation state of the solid skeleton is the effective force state, defined as

$$\overline{\underline{\boldsymbol{T}}} = \underline{\boldsymbol{T}} - B\left(\psi^{w}\underline{\boldsymbol{T}}_{w} + \psi^{a}\underline{\boldsymbol{T}}_{a}\right). \tag{73}$$

Since $\psi^{w} + \psi^{a} = 1$, it follows that

$$\overline{\underline{\mathbf{T}}} = \underline{\mathbf{T}} - B\left(\psi^{w}\underline{\mathbf{T}}_{w} + (1-\psi^{w})\underline{\mathbf{T}}_{a}\right) = \underline{\mathbf{T}} - B\underline{\mathbf{T}}_{a} + \psi^{w} B\left(\underline{\mathbf{T}}_{a} - \underline{\mathbf{T}}_{w}\right). \tag{74}$$

The effective force state $\overline{\underline{\boldsymbol{T}}}$ can be thought of as a constitutive force state in the sense that it can be determined by a peridynamic constitutive model given the deformation state as shown in the following section. Physically, the effective force state is the portion of the total force state imposed on the skeleton. In this sense, the effective force state concept can be utilized to model the mechanical behavior of deformable unsaturated porous media as an equivalent single-phase single-force-state material. Furthermore, we can define the net force state $\underline{\boldsymbol{T}}_{net}$ and the suction force state $\underline{\boldsymbol{T}}_{suct}$ as follows,

$$\underline{\boldsymbol{T}}_{net} = \underline{\boldsymbol{T}} - B\underline{\boldsymbol{T}}_{a}, \tag{75}$$

$$\underline{\boldsymbol{T}}_{suct} = -\left(\underline{\boldsymbol{T}}_{a} - \underline{\boldsymbol{T}}_{w}\right). \tag{76}$$

By assuming $B \approx 1$ (e.g., soils) (Terzaghi et al., 1996) the net force state degenerates into $\underline{\boldsymbol{T}} - \underline{\boldsymbol{T}}_{a}$. In this case, the net force state and the suction force state are analogous to the net stress and matric suction in classical unsaturated poromechanics for soils (e.g., Alonso et al., 1990; Fredlund and Morgenstern, 1977; Lu and Likos, 2004). It follows from (74) and (76) that

$$\overline{\underline{\boldsymbol{T}}} = \underline{\boldsymbol{T}} - B\underline{\boldsymbol{T}}_{a} - B\psi^{w}\underline{\boldsymbol{T}}_{suct}. \tag{77}$$

The effective force state distinguishes from the effective stress tensor in classical poromechanics in that the former is an energy-conjugate to the rate of nonlocal deformation state vector. From (77) the total force state of the whole porous medium can be expressed as

$$\underline{\boldsymbol{T}} = \overline{\underline{\boldsymbol{T}}} + B\underline{\boldsymbol{T}}_{a} + B\psi^{w}\underline{\boldsymbol{T}}_{suct}. \tag{78}$$

The second term of (71) can be expressed as

$$\sum_{\alpha=w,a}(1-\phi^s)\frac{\mathrm{d}\psi^\alpha}{\mathrm{d}t}p_\alpha=-(1-\phi^s)\dot{\psi}^w s \tag{79}$$

where $(1-\phi_s)$ represents the volume fraction of pore voids, and $s=p_a-p_w$ is matric suction in unsaturated porous media. The second term of (71) demonstrates that the quantity that is a work conjugate to matric suction s is $-(1-\phi^s)\dot{\psi}^w$. Mathematically it implies a functional relationship between matric suction, the volume fraction of pore space, and the degree of water saturation under isothermal conditions. This functional relationship is the water retention curve or soil-water characteristic curve in unsaturated soil mechanics (e.g., Cao et al., 2018; Song and Borja, 2014a, 2014b). The theoretical implication of this result is that the classical water retention curve still applies in unsaturated peridynamic poromechanics. Following the reasoning in Houlsby (1997), the first two terms of (71) also implies that the force states of deformable unsaturated porous media can be characterized by the net force state and matric suction force state as defined previously. The third term of (71) implies that pore fluid pressure is an energy conjugate to the rate of nonlocal volumetric fluid flow. And the fourth term of (71) represents the effect of the intrinsic compressibilities of pore fluid phases.

Substituting (78) into (26) the equation of motion for deformable unsaturated porous media (e.g., soil-like materials) can be written as

$$\int_{\mathcal{H}}\left[\left(\overline{\underline{\boldsymbol{T}}}+B\underline{\boldsymbol{T}}_a+B\psi^w\underline{\boldsymbol{T}}_{suct}\right)-\left(\overline{\underline{\boldsymbol{T}}}'+B\underline{\boldsymbol{T}}'_a+B\psi^w\underline{\boldsymbol{T}}'_{suct}\right)\right]\mathrm{d}V'+\rho(\boldsymbol{g}-\boldsymbol{a})-\sum_{\alpha=w,a}\rho^\alpha\tilde{\boldsymbol{a}}_\alpha=\boldsymbol{0}, \tag{80}$$

where the second term in the integrand is evaluated at point $\boldsymbol{x}'$. For the unsaturated poromechanics in geotechnical engineering, it is usually assumed that the pore air pressure in unsaturated geomaterials is atmospheric pressure (Zienkiewicz et al., 1999). Therefore, under quasi-static condition Eq. (80) can be simplified as

$$\int_{\mathcal{H}}\left[\left(\overline{\underline{\boldsymbol{T}}}+B\psi^w\underline{\boldsymbol{T}}_w\right)-\left(\overline{\underline{\boldsymbol{T}}}'+B\psi^w\underline{\boldsymbol{T}}'_w\right)\right]\mathrm{d}V'+\rho\boldsymbol{g}=\boldsymbol{0}. \tag{81}$$

In the fully saturated regime, we have $\psi^a=0$ and $\psi^w=1$. Thus, in this case, the effective force state reduces to

$$\overline{\underline{\boldsymbol{T}}}=\underline{\boldsymbol{T}}-B\underline{\boldsymbol{T}}_w. \tag{82}$$

3.2. Thermodynamic restrictions - reduced dissipation inequality

The second law of thermodynamics is about the entropy inequality principle. Without loss of generality, we assume no heat flux and heat source in three-phase porous media. Let η be the total entropy density per unit current volume of the three-phase porous media. The Clausius-Duhem inequality (Coleman and Noll, 1974) then reads

$$\theta\dot{\eta}\geq 0, \tag{83}$$

where θ is the absolute temperature. Now we define the free energy density per unit current volume by

$$W=\varepsilon-\theta\eta. \tag{84}$$

Here we assume that the free energy function W is representative of the total three-phase porous media and that it is associated with a material point attached to the solid matrix. It is noted that the functional form for W reflects the multiphase nature of the problem and depends on the specific form of the terms comprising the internal energy density ε. For isothermal processes, taking the time derivative of (84) leads to

$$\dot{W}=\dot{\varepsilon}-\theta\dot{\eta}. \tag{85}$$

Substituting (64) together with (65) into (85), it follows that

$$\dot{W}=\sum_{\alpha=s,w,a}\underline{\boldsymbol{T}}_{\alpha\alpha}\bullet\underline{\dot{\boldsymbol{Y}}}_{\alpha\alpha}-\theta\dot{\eta}. \tag{86}$$

Combining (86) and (83) yields the dissipation inequality

$$\mathscr{D}:=\theta\dot{\eta}=\sum_{\alpha=s,w,a}\underline{\boldsymbol{T}}_{\alpha\alpha}\bullet\underline{\dot{\boldsymbol{Y}}}_{\alpha\alpha}-\dot{W}\geqslant 0. \tag{87}$$

Applying the effective force state concept developed in the previous section, the dissipation inequality can be rewritten as

$$\mathscr{D}=\overline{\underline{\boldsymbol{T}}}\bullet\underline{\dot{\boldsymbol{Y}}}_{ss}+\sum_{\alpha=w,a}\left[\frac{1}{\rho_\alpha}\left(\rho_\alpha\phi^\alpha\bullet\underline{\dot{\vartheta}}_{\alpha\alpha}\right)-\left(\phi^\alpha\bullet\underline{\dot{\vartheta}}_{\alpha\alpha}\right)\right]p_\alpha+(1-\phi^s)s\dot{\psi}^w+\sum_{\alpha=w,a}\dot{\vartheta}^\alpha p_\alpha-\dot{W}\geqslant 0, \tag{88}$$

where $\overline{\underline{\boldsymbol{T}}}$ is the constitutive effective force state defined in the previous section, $\underline{\dot{\boldsymbol{Y}}}_{ss}$ is the rate of deformation state of the solid skeleton as defined before, and $\dot{\vartheta}^\alpha=\phi^\alpha\dot{p}_\alpha/K_\alpha$ for $\alpha=w,a$. The deformation state of the solid skeleton is assumed to be decomposed into the

elastic part and the inelastic part. Its rate form reads

$$\dot{\underline{\boldsymbol{Y}}}_{ss} = \dot{\underline{\boldsymbol{Y}}}^{e}_{ss} + \dot{\underline{\boldsymbol{Y}}}^{p}_{ss}. \tag{89}$$

Similarly, $\dot{\vartheta}^{\alpha}$ is assumed to be decomposed into the elastic part and the inelastic part as

$$\dot{\vartheta}^{\alpha} = \dot{\vartheta}^{\alpha,e} + \dot{\vartheta}^{\alpha,p}. \tag{90}$$

We now assume a free energy function in the form

$$W = W\left(\underline{\boldsymbol{Y}}^{e}_{ss}, \tilde{\underline{\boldsymbol{Y}}}_{ww}, \tilde{\underline{\boldsymbol{Y}}}_{\alpha\alpha}, \vartheta^{w,e}, \vartheta^{\alpha,e}, \boldsymbol{\zeta}\right), \tag{91}$$

where $\boldsymbol{\zeta}$ stands for the usual vector of plastic internal variables. Hence $\dot{W}$ involves the Fréchet derivatives of W with respect to $\underline{\boldsymbol{Y}}^{e}_{ss}$, $\tilde{\underline{\boldsymbol{Y}}}_{ww}$ and $\tilde{\underline{\boldsymbol{Y}}}_{\alpha\alpha}$. Taking the time derivative gives

$$\dot{W} = \frac{\partial W}{\partial \underline{\boldsymbol{Y}}^{e}_{ss}} \bullet \dot{\underline{\boldsymbol{Y}}}^{e}_{ss} + \sum_{\alpha=w,a} \frac{\partial W}{\partial \tilde{\underline{\boldsymbol{Y}}}_{\alpha\alpha}} \bullet \dot{\tilde{\underline{\boldsymbol{Y}}}}_{\alpha\alpha} + \sum_{\alpha=w,a} \frac{\partial W}{\partial \vartheta^{\alpha,e}} \dot{\vartheta}^{\alpha,e} + \frac{\partial W}{\partial \boldsymbol{\zeta}} \cdot \dot{\boldsymbol{\zeta}}. \tag{92}$$

Substituting (92) into (88) gives

$$\mathscr{D} = \left(\overline{\underline{\boldsymbol{T}}} - \frac{\partial W}{\partial \underline{\boldsymbol{Y}}^{e}_{ss}}\right) \bullet \dot{\underline{\boldsymbol{Y}}}^{e}_{ss} + \sum_{\alpha=w,a} \left(\underline{\boldsymbol{g}}_{\alpha} - \frac{\partial W}{\partial \tilde{\underline{\boldsymbol{Y}}}_{\alpha\alpha}}\right) \bullet \dot{\tilde{\underline{\boldsymbol{Y}}}}_{\alpha\alpha} + \sum_{\alpha=w,a} \left(p_{\alpha} - \frac{\partial W}{\partial \vartheta^{\alpha,e}}\right) \dot{\vartheta}^{\alpha,e} + \overline{\underline{\boldsymbol{T}}} \bullet \dot{\underline{\boldsymbol{Y}}}^{p}_{ss} - s(1-\phi^{s})\dot{\psi}^{w} + \sum_{\alpha=w,a} p_{\alpha}\dot{\vartheta}^{\alpha,p} + \boldsymbol{q} \cdot \dot{\boldsymbol{\zeta}} \geqslant 0, \tag{93}$$

where $\underline{\boldsymbol{g}}_{\alpha}$ is the equivalent Gibbs potential for pore fluid α per unit current volume of the mixture in peridynamics, and $\boldsymbol{q} = -\frac{\partial W}{\partial \boldsymbol{\zeta}}$. In principle, $\dot{\underline{\boldsymbol{Y}}}^{e}_{ss}$, $\dot{\tilde{\underline{\boldsymbol{Y}}}}_{\alpha\alpha}$ and $\dot{\vartheta}^{\alpha,e}$ can vary independently. Thus, the argument of Coleman and Noll (1974) yields the following constitutive relationships.

$$\overline{\underline{\boldsymbol{T}}} = \frac{\partial W}{\partial \underline{\boldsymbol{Y}}^{e}_{ss}}, \quad \underline{\boldsymbol{g}}_{\alpha} = \left.\frac{\partial W}{\partial \tilde{\underline{\boldsymbol{Y}}}_{\alpha\alpha}}\right|_{\alpha=w,a}, \quad p_{\alpha} = \left.\frac{\partial W}{\partial \vartheta^{\alpha,e}}\right|_{\alpha=w,a}. \tag{94}$$

The first constitutive equation implies that the effective force state $\overline{\underline{\boldsymbol{T}}}$ can be determined by the elastic deformation state of the solid skeleton through an elastic functional relation. Substituting (94) into (93) yields the reduced local dissipation function

$$\mathscr{D} = \overline{\underline{\boldsymbol{T}}} \bullet \dot{\underline{\boldsymbol{Y}}}^{p}_{ss} - s(1-\phi^{s})\dot{\psi}^{w} + \sum_{\alpha=w,a} p_{\alpha}\dot{\vartheta}^{\alpha,p} + \boldsymbol{q} \cdot \dot{\boldsymbol{\zeta}} \geqslant 0. \tag{95}$$

The above formulation does not comprise a constitutive constraint on the degree of saturation of water ψ^{w}. Thus we may postulate appropriate flow rules for the rate variables $\dot{\underline{\boldsymbol{Y}}}^{p}$, $\dot{\psi}^{w}$, $\dot{\vartheta}^{\alpha,p}$, and $\dot{\boldsymbol{\zeta}}$ in peridynamics. It is evident that the second law of thermodynamics identifies a complete effective force state $\overline{\underline{\boldsymbol{T}}}$ necessary to satisfy the entropy production inequality. Given the effective force state and the deformation state of the solid skeleton of deforming unsaturated porous media a peridynamic elastoplastic material model can be formulated for unsaturated porous media following the lines in Silling et al. (2007).

4. Multiphase constitutive correspondence principle

In this section, the multiphase constitutive correspondence principle is formulated to incorporate the well-established coupled poromechanics constitutive models in classical theory into unsaturated peri-poromechanics. In the state-based peridynamics theory, a constitutive model provides a vector state or a scalar state (*force state* or *mass flow state*) as a function of another vector state or scalar state (*deformation state* or *fluid potential state*). However, in classical unsaturated poromechanics, a constitutive model specifies a tensor or vector (stress or fluid flux) as a function of another tensor or vector (strain or fluid pressure gradient). Thus, it is necessary to define the peridynamic gradients of the deformation state of the skeleton and the fluid potential state, respectively. In this regard, the least square weighted residual technique is applied to derive peridynamic gradients of the skeleton deformation and fluid potential states. Then the energy equivalence method is utilized to establish the multiphase constitutive correspondence principle for the coupled solid deformation and unsaturated fluid flow processes.

4.1. Nonlocal peridynamic gradients of the skeleton deformation and fluid potential states

This part concerns the nonlocal peridynamic deformation gradient and the nonlocal peridynamic pressure gradient at point $\boldsymbol{x}$ from kinematic and internal state quantities, $\underline{\boldsymbol{Y}}_{ss}$ - the deformation state of the solid skeleton and $\underline{\Phi}_{\alpha}$ - the potential state of fluid phase α. We use Taylor series expansion of the deformation state at the point $\boldsymbol{x}$,

$$\underline{\boldsymbol{Y}}_{ss} = \boldsymbol{y}_s(\boldsymbol{x}') - \boldsymbol{y}_s(\boldsymbol{x}) = \boldsymbol{\xi} \cdot \nabla \boldsymbol{y}_s[\boldsymbol{x}] + \mathcal{O}(\parallel \boldsymbol{\xi} \parallel^2) \tag{96}$$

We define the nonlocal peridynamic deformation gradient $\widetilde{\boldsymbol{F}} = \nabla \boldsymbol{y}_s$, using the least square weighted residual technique such that $\widetilde{\boldsymbol{F}} \cdot \boldsymbol{\xi}$ gives the best approximation to $\underline{\boldsymbol{Y}}_{ss}$ in a weighted L2 norm generates

$$\frac{\partial}{\partial \widetilde{\boldsymbol{F}}} \int_{\mathcal{H}} \underline{\omega} \left(\underline{\boldsymbol{Y}}_{ss} - \widetilde{\boldsymbol{F}} \cdot \boldsymbol{\xi} \right)^2 \mathrm{d}V' = 0. \tag{97}$$

Conducting the derivative evaluation on a component-by-component basis yields

$$\int_{\mathcal{H}} \underline{\omega}\, \underline{\boldsymbol{Y}}_{ssj} \xi_l \mathrm{d}V' - \widetilde{\boldsymbol{F}}_{ji} \int_{\mathcal{H}} \underline{\omega}\, \xi_i \xi_l \mathrm{d}V' = 0, \tag{98}$$

where $i,j,l = 1,2,3$. By solving Eq. (98), we obtain $\widetilde{\boldsymbol{F}}$

$$\widetilde{\boldsymbol{F}}_{ij} = \int_{\mathcal{H}} \underline{\omega}\, \underline{\boldsymbol{Y}}_{ssj} \xi_l \mathrm{d}V' \left(\int_{\mathcal{H}} \underline{\omega}\, \xi_i \xi_l \mathrm{d}V' \right)^{-1}. \tag{99}$$

In the tensorial form

$$\widetilde{\boldsymbol{F}} = \int_{\mathcal{H}} \underline{\omega}\, \underline{\boldsymbol{Y}}_{ss} \otimes \boldsymbol{\xi} \mathrm{d}V' \left(\int_{\mathcal{H}} \underline{\omega}\, \boldsymbol{\xi} \otimes \boldsymbol{\xi} \mathrm{d}V' \right)^{-1}, \tag{100}$$

where $\otimes$ is the tensor product. As in the stated-based peridynamics, the shape tensor $\boldsymbol{K}$ of the bond $\boldsymbol{x}' - \boldsymbol{x}$ is

$$\boldsymbol{K} = \int_{\mathcal{H}} \underline{\omega}\, \boldsymbol{\xi} \otimes \boldsymbol{\xi} \mathrm{d}V' \tag{101}$$

Then the nonlocal peridynamic deformation gradient in a concise form is

$$\widetilde{\boldsymbol{F}}\left(\underline{\boldsymbol{Y}}_{ss} \right) = \left(\underline{\boldsymbol{Y}}_{ss} * \boldsymbol{\xi} \right) \boldsymbol{K}^{-1}. \tag{102}$$

The fluid flow potential state for fluid phase α on a bond $\boldsymbol{\xi} = \boldsymbol{x}' - \boldsymbol{x}$ can be defined as,

$$\underline{\Phi}_{\alpha} = \Phi'_{\alpha} - \Phi_{\alpha}, \tag{103}$$

where $\alpha = w, a$. By Taylor series expansion the fluid potential state of the pore fluid phase α at the point $\boldsymbol{x}$ can be written as

$$\underline{\Phi}_{\alpha} = \Phi'_{\alpha} - \Phi_{\alpha} = \boldsymbol{\xi} \cdot \nabla \Phi_{\alpha} + \mathcal{O}(\parallel \boldsymbol{\xi} \parallel^2) \tag{104}$$

We define the nonlocal peridynamic fluid potential gradient $\widetilde{\nabla} \Phi_{\alpha} = \nabla \Phi_{\alpha}$. Similarly, through the least square weighted residual technique we can derive the nonlocal peridynamic fluid potential gradient for pore fluid phase α at point $\boldsymbol{x}$ as

$$\widetilde{\nabla} \Phi_{\alpha} = \left(\underline{\omega}\, \underline{\Phi}_{\alpha} \bullet \boldsymbol{\xi} \right) \boldsymbol{K}^{-1}, \quad \text{with} \quad \alpha = w, a. \tag{105}$$

It can be proved that the approximate deformation and fluid potential gradients are exact if the deformation of the solid skeleton and the fluid potential states are homogeneous. Meanwhile, it is worth noting that the following Eqs. (96) and (104) the gradients of the solid deformation and fluids potential states at point $\boldsymbol{x}$ can be formulated with a high-order precision by incorporating the higher-order terms of their Taylor expansions.

4.2. Correspondence principle for the deformation of the solid skeleton

Constitutive modeling within the state-based peridynamic theory considers the collective deformation or fluid potentials of all the material within a neighborhood of point $\boldsymbol{x} \in \mathcal{B}$, where $\mathcal{B}$ is the reference configuration of the body. The deformation vector state $\underline{\boldsymbol{Y}}_{ss}$ represents a more general way of describing how a skeleton deforms locally than the classical concept of a deformation gradient tensor $\boldsymbol{F}$. However, given $\underline{\boldsymbol{Y}}_{ss}$ the corresponding nonlocal peridynamic deformation gradient tensor can be obtained by Eq. (102). A peridynamic constitutive model for the solid skeleton *corresponds* to the classical constitutive model for the solid skeleton at the nonlocal

peridynamic deformation gradient $\widetilde{\boldsymbol{F}}$, if

$$W\left(\underline{\boldsymbol{Y}}_{ss}\right) = \Omega\left(\widetilde{\boldsymbol{F}}\right), \tag{106}$$

where W is the peridynamic strain energy density function and Ω is the classical strain energy density function for the solid skeleton, respectively. Given $\widetilde{\boldsymbol{F}}$, we can obtain the effective Piola stress $\overline{\boldsymbol{P}}$ on the solid skeleton through a classical elastoplastic or visco-elastoplastic constitutive models for the solid skeleton in classical unsaturated poromechanics (e.g., Borja et al., 2013; Borja and Tamagnini, 1998; Nova et al., 2003; Simo and Hughes, 1999; Song, 2017). First, the Fréchet derivative of $\widetilde{\boldsymbol{F}}$ is

$$\left(\nabla\widetilde{F}\right)_{ijk}\left(\underline{\boldsymbol{Y}}_{ss}\right) = \delta_{ik}\underline{\omega}\, K^{-1}_{pj}\xi_p. \tag{107}$$

It is noted that $\nabla\widetilde{\boldsymbol{F}}$ is a state of order 3. The incremental change in W due to an incremental change in $\underline{\boldsymbol{Y}}_{ss}$ is

$$\begin{aligned}\Delta W &= \frac{\partial\Omega}{\partial\widetilde{F}_{ij}}\Delta\widetilde{F}_{ij}\\ &= \frac{\partial\Omega}{\partial\widetilde{F}_{ij}}\nabla\widetilde{F}_{ijk}\bullet\Delta y_{s,k}\\ &= \left(\overline{P}_{ij}\delta_{ik}\underline{\omega}\, K^{-1}_{pj}x_p\right)\bullet\Delta y_{s,k} = \left(\overline{P}_{kj}\underline{\omega}\, K^{-1}_{pj}x_p\right)\bullet\Delta y_{s,k},\end{aligned} \tag{108}$$

where $\overline{P}_{ij}$ is the effective Piola stress tensor of the solid skeleton. In the line with the state-based peridynamics for the solid material, the effective force state of the solid skeleton can be defined as

$$\underline{\overline{\boldsymbol{T}}} = \nabla W\left(\underline{\boldsymbol{Y}}_{ss}\right). \tag{109}$$

Comparing (108) and (109), we can get the effective force state on the solid skeleton as

$$\underline{\overline{\boldsymbol{T}}} = \underline{\omega}\,\overline{\boldsymbol{P}}\boldsymbol{K}^{-1}\boldsymbol{\xi}, \tag{110}$$

where $\overline{\boldsymbol{P}} = J\overline{\boldsymbol{\sigma}}\widetilde{\boldsymbol{F}}^{-T}$, $J = \det(\widetilde{\boldsymbol{F}})$, and $\overline{\boldsymbol{\sigma}}$ is the effective stress tensor as introduced in Appendix B. Substituting (156) in Appendix B into (110), the effective force state on the solid skeleton becomes

$$\underline{\overline{\boldsymbol{T}}} = \underline{\omega}\,[\boldsymbol{\sigma} + B(\psi^w p_w + \psi^a p_a)\boldsymbol{I}]J\widetilde{\boldsymbol{F}}^{-T}\boldsymbol{K}^{-1}\boldsymbol{\xi}, \tag{111}$$

where $\boldsymbol{\sigma}$ is the total stress tensor as introduced in Appendix B.

Through comparing (111) with (73), the total force state for unsaturated porous media and the 'intrinsic' force states for the pore water and pore air can be written as follows.

$$\underline{\boldsymbol{T}} = \underline{\omega}\, J\boldsymbol{\sigma}\widetilde{\boldsymbol{F}}^{-T}\boldsymbol{K}^{-1}\boldsymbol{\xi}, \tag{112}$$

$$\underline{\boldsymbol{T}}_w = -\underline{\omega}\, J\boldsymbol{I}p_w\widetilde{\boldsymbol{F}}^{-T}\boldsymbol{K}^{-1}\boldsymbol{\xi}, \tag{113}$$

$$\underline{\boldsymbol{T}}_a = -\underline{\omega}\, J\boldsymbol{I}p_a\widetilde{\boldsymbol{F}}^{-T}\boldsymbol{K}^{-1}\boldsymbol{\xi}. \tag{114}$$

It follows from (76) that the suction force state can be expressed as

$$\underline{\boldsymbol{T}}_{suct} = \underline{\omega}\, J\boldsymbol{I}(p_a - p_w)\widetilde{\boldsymbol{F}}^{-T}\boldsymbol{K}^{-1}\boldsymbol{\xi}. \tag{115}$$

Through (112), the equation of motion (80) can be rewritten as

$$\int_{\mathcal{H}}\left(\underline{\omega}\boldsymbol{\sigma}J\widetilde{\boldsymbol{F}}^{-T}\boldsymbol{K}^{-1}\boldsymbol{\xi} - \underline{\omega}\boldsymbol{\sigma}' J\widetilde{\boldsymbol{F}}^{-T}\boldsymbol{K}^{-1}\boldsymbol{\xi}'\right)\mathrm{d}V' + \rho(\boldsymbol{g}-\boldsymbol{a}) - \sum_{\alpha=\mathrm{w,a}}\rho^\alpha\tilde{\boldsymbol{a}}_\alpha = \boldsymbol{0}, \tag{116}$$

where the second term in the integrand is evaluated at point $\boldsymbol{x}'$. Through (116) the classical constitutive theory (e.g. Alonso et al., 1990; Cui and Delage, 1996; Gallipoli et al., 2003; Gens, 2010; Song et al., 2018a, 2018b; Wheeler and Sivakumar, 1995) can be cast in peridynamics to model the mechanical behavior of unsaturated porous media. It shall be noted that the non-local material model formulated in this way can include dependencies such as time, rate, and history.

4.3. Correspondence principle for unsaturated fluid flow

This part concerns the correspondence principle for unsaturated fluid flow in porous media. From classical unsaturated poromechanics, the mass flux at point $\boldsymbol{x}$ equals to the product of fluid density ρ_α and volumetric flux $\boldsymbol{q}_\alpha$ ($\alpha = w, a$), which is determined by the generalized Darcy's law for unsaturated fluid flow. We define the peridynamic correspondence principle for the unsaturated fluid flow in porous media as that the peridynamic fluid flow model corresponds to the generalized Darcy's law at $\widetilde{\nabla}\Phi_\alpha$ with $\alpha = w, a$, if

$$W\left(\underline{\Phi}_\alpha\right) = \Omega(\widetilde{\nabla}\Phi_\alpha), \tag{117}$$

where $W(\underline{\Phi}_\alpha)$ is the peridynamic dissipation energy density function of the fluid flow, and $\Omega(\widetilde{\nabla}\Phi_\alpha)$ is the classical dissipation energy density function for the fluid flow. Refer to the generalized Darcy's law for two-phase fluid flow in porous media (e.g., Coussy, 2004; Lewis and Schrefler, 1998; Song et al., 2017; Wang and Song, 2020). Given the peridynamic fluid potential gradients in (105) at point $\boldsymbol{x}$ we propose the peridynamic volume flux for the fluid phases as

$$\boldsymbol{q}_\alpha = -\frac{k_\alpha^r \kappa}{\mu_\alpha}\left(\underline{\omega}\,\underline{\Phi}_\alpha \bullet \boldsymbol{\xi}\right)\boldsymbol{K}^{-1}, \tag{118}$$

where k_α^r is the relative permeability of pore fluid α in classical unsaturated poromechanics, κ is the saturated permeability of the solid skeleton, and μ_α is the viscosity of pore fluid α. Next, referring to (105) the Fréchet derivative of $\nabla\Phi_\alpha$ with respect to Φ_α is

$$(\nabla\nabla\Phi_\alpha)_j(\Phi_\alpha) = \underline{\omega}\,K_{pj}^{-1}\xi_p. \tag{119}$$

Then the incremental change in $W(\underline{\Phi}_\alpha)$ due to an incremental change in $\underline{\Phi}_\alpha$ is

$$\begin{aligned}\Delta W\left(\underline{\Phi}_\alpha\right) &= \frac{\partial\Omega}{\partial\widetilde{\nabla}\Phi_{\alpha,i}}\Delta(\widetilde{\nabla}\Phi)_{\alpha,i}\\ &= \frac{\partial\Omega}{\partial\widetilde{\nabla}\Phi_{\alpha,i}}\nabla(\widetilde{\nabla}\Phi)_{\alpha,i}\bullet\Delta\Phi_\alpha\\ &= \left(Jq_{\alpha,i}\underline{\omega}\,K_{ji}^{-1}x_j\right)\bullet\Delta\Phi_\alpha.\end{aligned} \tag{120}$$

Next, in line with the state-based peridynamics the mass flow state for the fluid phases can be defined as

$$\underline{Q}_\alpha = \nabla W\left(\underline{\Phi}_\alpha\right). \tag{121}$$

Comparing (121) and (120) we can define the mass flow state for the fluid phases at point $\boldsymbol{x}$ as

$$\underline{Q}_\alpha = \underline{\omega}\,\rho_\alpha J\boldsymbol{q}_\alpha\boldsymbol{K}^{-1}\boldsymbol{\xi}. \tag{122}$$

Substituting (122) into (43), the mass balance equations for the fluid phases can be rewritten as

$$(1-\phi^s)\frac{\mathrm{d}\psi^\alpha}{\mathrm{d}t} + \frac{\phi^\alpha}{K_\alpha}\frac{\mathrm{d}p_\alpha}{\mathrm{d}t} + \psi^\alpha B\int_{\mathcal{H}}\left(\underline{\omega}\,\boldsymbol{v}_s'\boldsymbol{K}^{-1}\boldsymbol{\xi}' - \underline{\omega}\,\boldsymbol{v}_s\boldsymbol{K}^{-1}\boldsymbol{\xi}\right)\mathrm{d}V' + \frac{1}{\rho_\alpha}\int_{\mathcal{H}}\left(\underline{\omega}\,\rho_\alpha J\boldsymbol{q}_\alpha'\boldsymbol{K}^{-1}\boldsymbol{\xi}' - \underline{\omega}\,\rho_\alpha J\boldsymbol{q}_\alpha\boldsymbol{K}^{-1}\boldsymbol{\xi}\right)\mathrm{d}V' = 0, \tag{123}$$

where the integral in the third term of Eq. (123) is obtained referring to the peridynamic approximation of the divergence operator on a vector (i.e., $\boldsymbol{v}_s$ in this case). In classical unsaturated poromechanics, the constitutive model for the solid skeleton and the generalized Darcy's law for unsaturated fluid flow are coupled through the soil-water retention curve (e.g., degree of saturation in the effective stress and relative permeability). Similarly, the effective force state and the unsaturated fluid flow state are also coupled through the multiphase constitutive correspondence principle formulated here.

5. Numerical examples through the effective force state concept

This section will test the hypothesis that the formulated effective force state concept can be utilized to model unsaturated porous media as *an equivalent single-phase single-force state peridynamic material*. For this purpose, the formation of shear banding in deformable unsaturated porous media will be simulated numerically by utilizing *the effective force state concept*. It is assumed that $B \approx 1$ (Terzaghi et al., 1996), the matric suction force state is given and constant, and pore air pressure is passive (e.g., atmospheric pressure). Note that the latter assumption is common in solving practical geomechanics problems (Zienkiewicz et al., 1999). Thus, the mass balance of fluid phases is uncoupled from the linear momentum balance. It follows that the equation of motion (116) under quasi-static condition degenerates into

$$\int_{\mathcal{H}}\left(\underline{\omega}\,\overline{\boldsymbol{\sigma}}\,J\widetilde{\boldsymbol{F}}^{-T}\boldsymbol{K}^{-1}\boldsymbol{\xi} - \underline{\omega}\,\overline{\boldsymbol{\sigma}}'J\widetilde{\boldsymbol{F}}^{-T}\boldsymbol{K}^{-1}\boldsymbol{\xi}'\right)\mathrm{d}V' + \rho\boldsymbol{g} = \boldsymbol{0}. \tag{124}$$

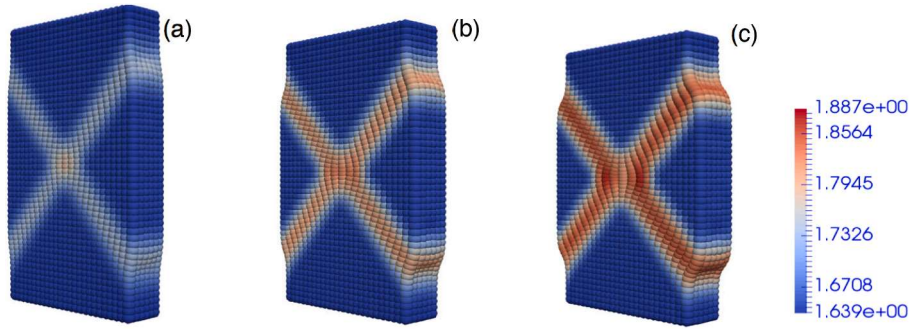

Fig. 3. Contours of specific volume in the sample with a suction of 30 kPa at three loading stages: (a) 3%, (b) 5.25%, and (c) 7.5%, respectively.

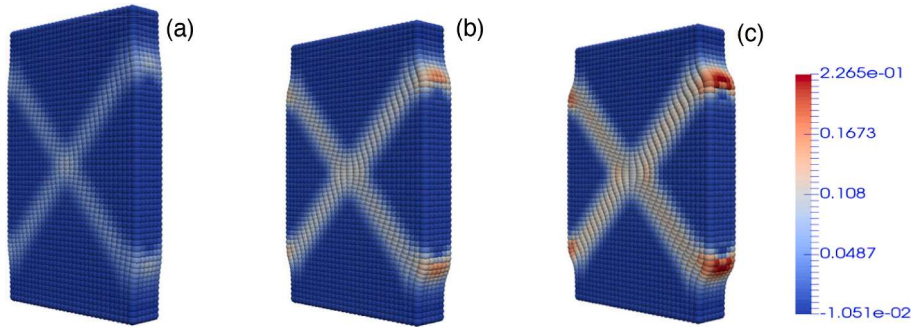

Fig. 4. Contours of plastic volumeric strain in the sample with a suction of 30 kPa at three loading stages: (a) 3%, (b) 5.25%, and (c) 7.5%, respectively.

Here, Eq. (124) is solved by a Lagrangian meshfree method formulated for the single-phase peridynamic material (Silling, 2004; Silling and Askari, 2005). For the numerical simulations presented below, $\overline{\boldsymbol{\sigma}}$ is determined through an elasto-plastic constitutive model for unsaturated soils in which the yielding function varies with plastic volumetric strain and matric suction (Borja et al., 2013). A brief summary of this material model is presented as follows.

Given the nonlocal deformation gradient, the total strain can be determined following the lines in continuum mechanics (Holzapfel, 2000). The total strain is decomposed into the elastic strain and the plastic strain which reads

$$\boldsymbol{\epsilon} = \boldsymbol{\epsilon}^e + \boldsymbol{\epsilon}^p, \tag{125}$$

where $\boldsymbol{\epsilon}^e$ and $\boldsymbol{\epsilon}^p$ are the elastic strain and the plastic strain, respectively. The effective stress tensor is determined by

$$\overline{\boldsymbol{\sigma}} = \mathcal{C}^e : \boldsymbol{\epsilon}^e, \tag{126}$$

where : stands for the double inner product operator and $\mathcal{C}^e$ is the isotropic elastic stiffness tensor that is expressed as

$$\mathcal{C}^e = \mathscr{K}^e \boldsymbol{I} \otimes \boldsymbol{I} + 2\mathscr{G}^e \left(\mathcal{I} - \frac{1}{3} \boldsymbol{I} \otimes \boldsymbol{I} \right), \tag{127}$$

where $\mathscr{K}^e$ and $\mathscr{G}^e$ are the elastic bulk and shear modulus respectively which can be determined by Young's modulus and Poisson ratio (Malvern, 1969), $\mathcal{I}$ is the fourth-order identity tensor, and $\otimes$ is the tensor product operator. The yield function f is determined by

$$f\left(p', q, \overline{p}_c\right) = \frac{q^2}{M^2} + \left(p' - \overline{p}_c\right) p' \leqslant 0, \tag{128}$$

where p' is the effective mean stress, q is the equivalent shear stress, M is the slope of the critical state line, and $\overline{p}_c$ is the apparent effective preconsolidation pressure. As a hardening law, $\overline{p}_c$ is written as

$$\overline{p}_c = -\exp(c_1)(-p_c)^{c_2}, \tag{129}$$

where c_1 and c_2 are two variables that evolve with matric suction and the degree of saturation of water (Borja, 2004; Borja et al., 2013), and p_c is the apparent preconsolidation pressure under saturated condition which evolves with plastic volumetric strain.

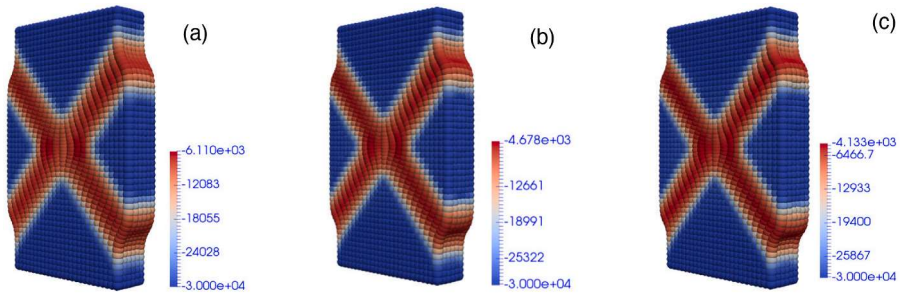

Fig. 5. Contours of the effective preconsolidation pressure of the simulations with suctions of (a) 20 kPa, (b) 30 kPa, and (c) 40 kPa respectively at the axial strain of 7.5%.

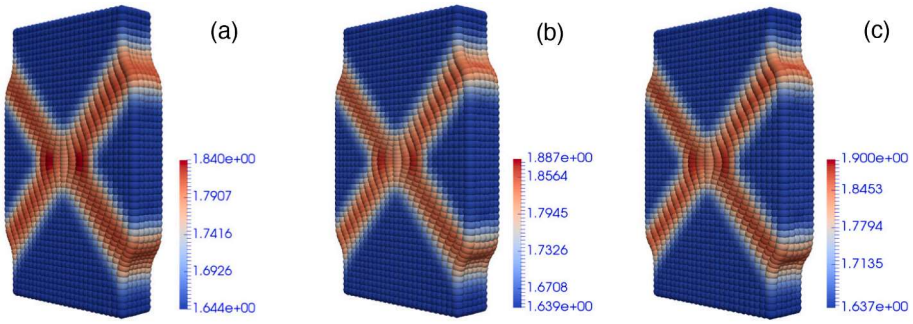

Fig. 6. Contours of the specific volume of the simulations with suctions of (a) 20 kPa, (b) 30 kPa, and (c) 40 kPa respectively at the axial strain of 7.5%.

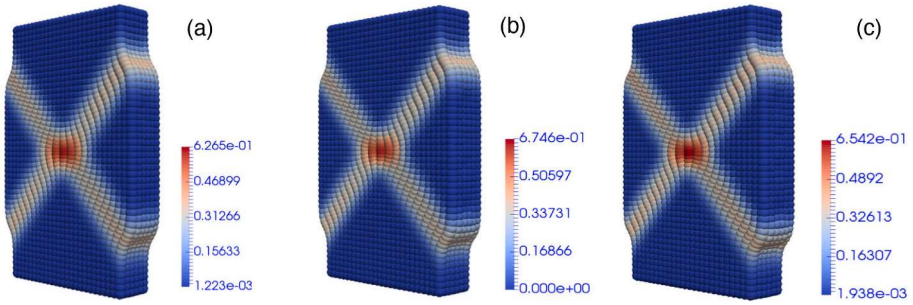

Fig. 7. Contours of the plastic shear strain of the simulations with matric suctions of (a) 20 kPa, (b) 30 kPa, and (c) 40 kPa respectively at the axial strain of 7.5%.

$$\dot{p}_c = \frac{-p_c}{\lambda - \kappa}\mathrm{tr}(\dot{\boldsymbol{\epsilon}}^p), \tag{130}$$

where λ and κ are the swelling index and the compression index, respectively. The plastic strain is determined by assuming the associative flow rule as follows.

$$\dot{\boldsymbol{\epsilon}}^p = \dot{\Lambda}\frac{\partial f}{\partial \overline{\boldsymbol{\sigma}}}, \tag{131}$$

where $\dot{\Lambda}$ is the plastic multiplier. This constitutive model is numerically implemented through the classic return-mapping algorithm (Borja, 2013; Simo and Hughes, 1999).

The material parameters are as follows. Young's modulus $E = 50$ MPa, Poisson ratio $\nu = 0.3$, the swelling index $\kappa = 0.03$, the critical state line slope $M = 1.0$, the compression index $\lambda = 0.11$, the soil density $\rho_s = 2600$ kg/m^3, the water density $\rho_w = 1000$ kg/m^3, and the initial porosity $\phi = 0.5$. The water degree of saturation is determined by the soil-water characteristic curve (Van Genuchten, 1980).

$$\psi^w = [1 + (s/s_a)^n]^{-m}, \tag{132}$$

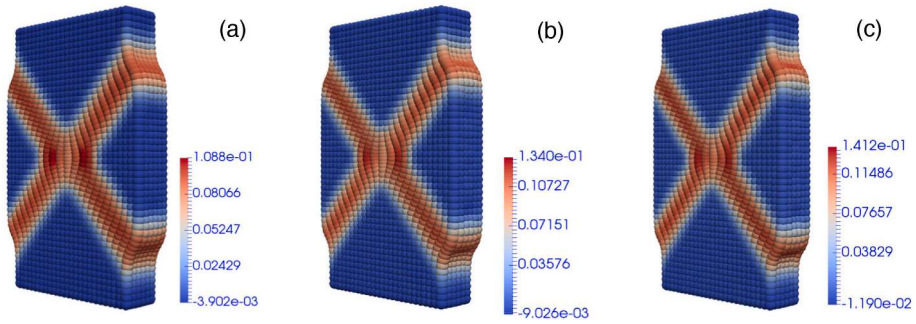

Fig. 8. Contours of the plastic volumetric strain of the simulations with matric suctions of (a) 20 kPa, (b) 30 kPa, and (c) 40 kPa respectively at the axial strain of 7.5%.

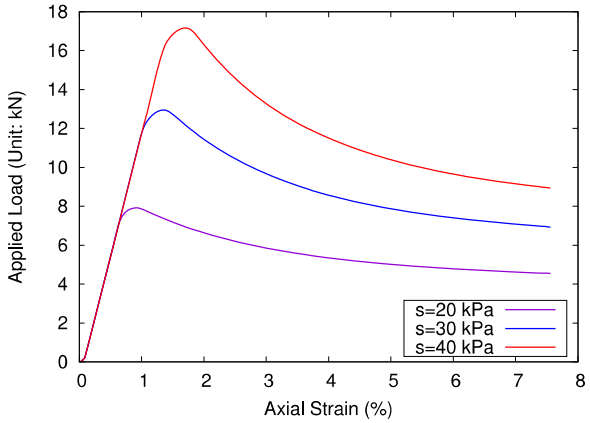

Fig. 9. Comparison of load curves of the simulations with matric suctions of (a) 20 kPa, (b) 30 kPa, and (c) 40 kPa respectively.

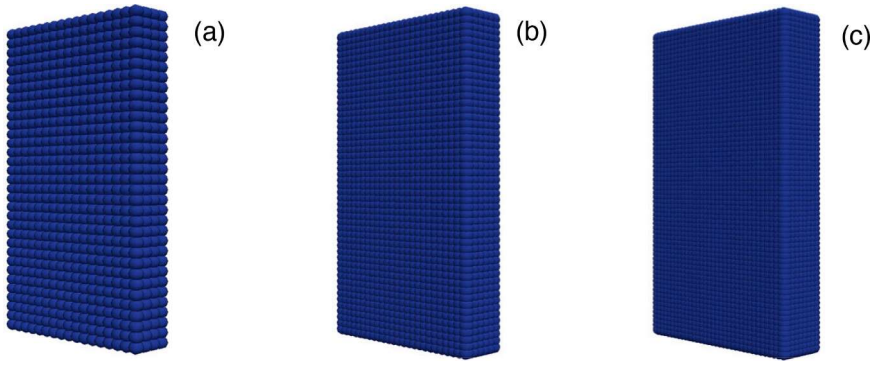

Fig. 10. Comparison of three spatial discretization schemes.

where s_a, n and m are material parameters. It is assumed that $s_a = 10$ kPa, $n = 2.0$, and $m = 0.5$. The unsaturated soil sample has a dimension of 10 cm $\times$ 20 cm $\times$ 2.4 cm in the x, y, and z directions. The sample is discretized into 7,500 equal-sized material points with a characteristic length $\Delta x = 0.4$ cm. The sample is restricted to deform in the x - y plane. The bottom boundary is fixed (i.e., zero displacements in the x and y directions). An effective force state that is equivalent to a constant confining pressure of 100 kPa is prescribed on both lateral boundaries in the $x - y$ plane. A vertical displacement load is applied on the top boundary at the rate of $v_y = 0.015$ cm/s. The final axial strain is 7.5%. As suggested in Silling and Askari (2005), the horizon is assumed as $3\Delta x$ (i.e., 1.2 cm). It is noted that the horizon may be chosen to characterize the physical length scale of deformable unsaturated porous media (e.g., the thickness of shear bands) (Song and Menon, 2018).

The results of the three simulations under different matric suctions are as follows. The results of the simulation under a matric suction of 30 kPa is presented first. Fig. 3 plots the contours of specific volume in the deformed configuration of the specimen at three

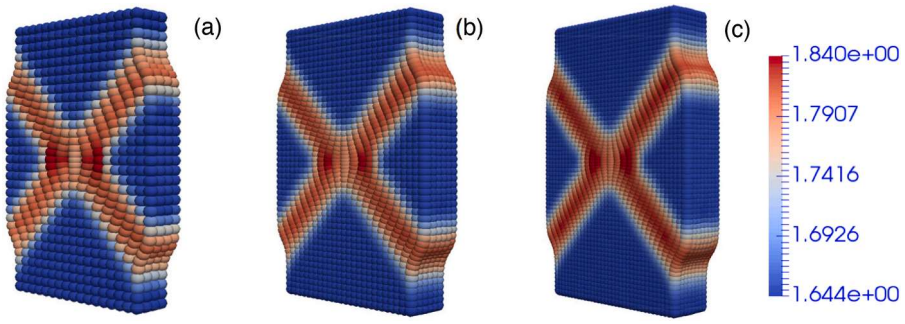

Fig. 11. Comparison of the contours of specific volume with the three spatial discretizations.

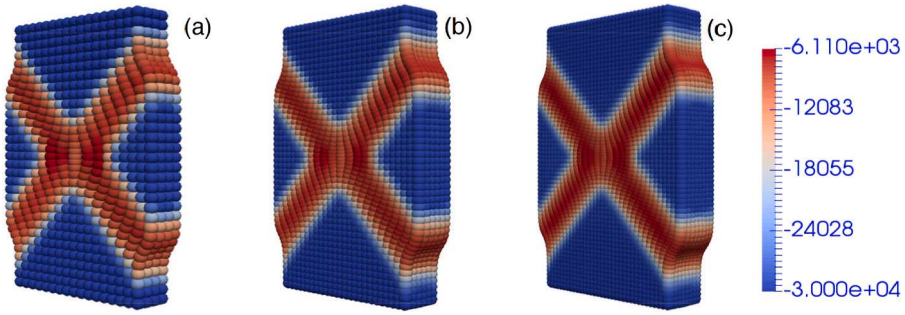

Fig. 12. Comparison of the contours of the effective preconsolidation pressure with the three spatial discretizations.

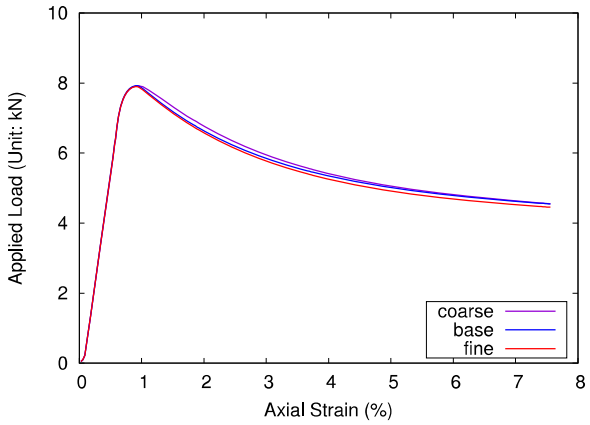

Fig. 13. Comparison of the load curves of the simulations with the three spatial discretizations.

loading stages. It is concluded from the contours of specific volume both shear bands are dilative since the specific volume increases from its initial value in shear bands. This conclusion is supported by the results in Fig. 4 that plots the contours of plastic volumetric strain at the same three loading stages. The results of the simulations under three different suctions are presented next. Figs. 5 and 6 compare the contours of effective preconsolidation pressure and specific volume in the deformed configurations at the axial strain of 7.5% for the three simulations, respectively. The results demonstrate that for all cases the magnitude of effective preconsolidation pressure decreases while the specific volume increases. Furthermore, the suction affects the value of effective preconsolidation pressure and the specific volume in the localized shear zones. The contours of plastic shear strain and plastic volumetric strain for the three simulations at the same axial strain are presented in Figs. 7 and 8, respectively. In the shear bands, both plastic shear strain and volumetric strain are influenced by matric suction. The load curves are plotted in Fig. 9. It is shown that the suction impacts the peak load capacity of the specimen. The results also show that the simulation with a larger matric suction shows a more evident strain-softening behavior.

A sensitivity analysis of the numerical results with respect to spatial discretization schemes is also presented. Three spatial discretization schemes, Case (a), Case (b), and Case (c) are plotted in Fig. 10. Case (a) consists of 2,244 material points. Case (b) consists of

7,500 material points. Case (c) consists of 17,952 material points. The same input material parameters, boundary conditions, loading protocol and horizon for the simulations above are adopted in this analysis. The sample under the matric suction of 30 kPa is rerun with the spatial discretization schemes in Case (a) and Case (c).

The contours of specific volume from the simulations with the three spatial discretization schemes at the axial strain of 7.5% are plotted in Figs. 11 and 12. It is shown that the contours of specific volume and effective preconsolidation pressure are almost identical at the same axial strain by the simulations with the three spatial discretization schemes. It may be concluded that the results are not sensitive to the spatial discretization scheme given the same horizon is used for all simulations. This conclusion is corroborated by the load curves in Fig. 13. The load curves for the three simulations are identical before the peak load. In the post-peak load regime, the load curves are slightly different. It is noted that an enhanced constitutive model incorporating the residual behavior of unsaturated porous media is needed to better simulate the residual loading capacity of such materials.

6. Summary

In this article, a multiphase correspondence principle is proposed and the effective force state is derived for modeling unsaturated deformable porous media as an equivalent single-phase and single-force state peridynamic material. The peridynamic linear momentum balance equation of unsaturated porous media is formulated by assuming a free energy density for the three-phase porous mixture, which is a function of the deformation and relative deformation states of the solid skeleton and pore fluids. Even though the procedure is general, the equations are valid for unsaturated soil-like materials. The dilation or volume states are applied to cast the mass balance equations for unsaturated porous media in peridynamics. The energy balance of unsaturated porous media is utilized to derive the effective force state for the solid skeleton, which is an energy conjugate to the nonlocal deformation state of the solid. Thus the effective force state distinguishes from the effective stress concept in classical unsaturated poromechanics. Through an energy equivalence, we have built a multiphase constitutive correspondence principle for unsaturated peri-poromechanics that extends the original constitutive correspondence principle for solid materials. The multiphase correspondence principle provides a means to incorporate advanced constitutive models that have been well-established in classical theory directly into unsaturated peri-poromechanics. Numerical simulations of localized failure in unsaturated porous media under different matric suctions are presented to show the feasibility of modeling the mechanical behavior of such materials as an equivalent single-phase and single-force state peridynamic material through the effective force state concept.

CRediT authorship contribution statement

Xiaoyu Song: Conceptualization, Methodology, Software, Funding acquisition. **Stewart A. Silling :** Conceptualization, Methodology, Software.

Declaration of Competing Interest

The authors declare that they have no known competing financial interests or personal relationships that could have appeared to influence the work reported in this paper.

Acknowledgments

Support for this work was provided by the US National Science Foundation (NSF) under contract numbers CMMI 1659932 and 1944009. The authors are grateful to the anonymous reviewers for their constructive reviews.

Appendix A. Peridynamic operators

Let $\underline{a}$ and $\underline{b}$ be scalar states and $\underline{\boldsymbol{A}}$ and $\underline{\boldsymbol{B}}$ be vector states. The *dot product* and *tensor product* are defined as follows

$$\underline{a} \bullet \underline{b} = \int_{\mathcal{H}} \underline{a}\langle \boldsymbol{\xi} \rangle \cdot \underline{b}\langle \boldsymbol{\xi} \rangle \mathrm{d}V_{\boldsymbol{x}'}, \tag{133}$$

$$\underline{\boldsymbol{A}} \bullet \underline{\boldsymbol{B}} = \int_{\mathcal{H}} \underline{\boldsymbol{A}}\langle \boldsymbol{\xi} \rangle \cdot \underline{\boldsymbol{B}}\langle \boldsymbol{\xi} \rangle \mathrm{d}V_{\boldsymbol{x}'}, \tag{134}$$

$$\underline{\boldsymbol{A}} * \underline{\boldsymbol{B}} = \int_{\mathcal{H}} \underline{\boldsymbol{A}}\langle \boldsymbol{\xi} \rangle \otimes \underline{\boldsymbol{B}}\langle \boldsymbol{\xi} \rangle \mathrm{d}V_{\boldsymbol{x}'}, \tag{135}$$

where the symbol $\cdot$ and $\otimes$ denote the inner product and tensor product of two vectors in $\mathbb{R}^3$. For brevity, in this article we adopt V and V' to represent the volumes of material points $\boldsymbol{x}$ and $\boldsymbol{x}'$, respectively. The norm of a scalar state or a vector state is defined by

$$\| \underline{a} \| = \sqrt{\underline{a} \bullet \underline{a}}, \quad \| \underline{\boldsymbol{A}} \| = \sqrt{\underline{\boldsymbol{A}} \bullet \underline{\boldsymbol{A}}}. \tag{136}$$

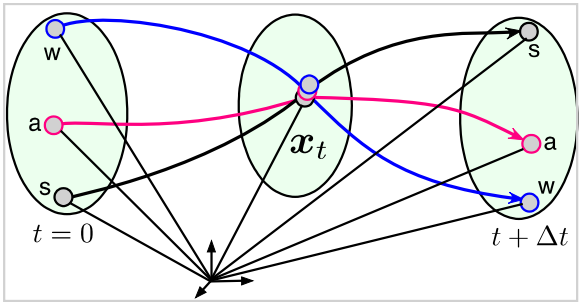

Fig. 14. Schematic of kinematics of three-phase porous media in classical unsaturated poromechanics.

If $\psi(\cdot):\mathcal{S}\to\mathbb{R}$ is a function of a scalar state, and $\Psi(\cdot):\mathcal{V}\to\mathbb{R}$ is a function of a vector state, their *Fréchet derivatives*, if they exist, are defined by

$$\psi\left(\underline{A}+\underline{a}\right)=\psi\left(\underline{A}\right)+\nabla\psi\left(\underline{A}\right)\bullet\underline{a}+\mathcal{O}(\|\underline{a}\|), \tag{137}$$

$$\Psi\left(\underline{\boldsymbol{A}}+\underline{\boldsymbol{a}}\right)=\Psi\left(\underline{\boldsymbol{A}}\right)+\nabla\Psi\left(\underline{\boldsymbol{A}}\right)\bullet\underline{\boldsymbol{a}}+\mathcal{O}(\|\underline{\boldsymbol{a}}\|), \tag{138}$$

where $\underline{A}$ and $\underline{a}$ are any scalar states, $\underline{\boldsymbol{A}}$ and $\underline{\boldsymbol{a}}$ are any vector states, $\nabla\psi$ is a scalar state, and $\nabla\Psi$ is a vector state.

Appendix B. Classical unsaturated poromechanics

We review the key notions and assumption in classical unsaturated poromechanics for deformable unsaturated porous media because they are used in formulating peridynamic unsaturated poromecahnics. Here unsaturated porous media means the porous material consists of a solid skeleton, and two immiscible fluids in the continuous pore space, e.g., unsaturated geomaterials (Fredlund and Rahardjo, 1993; Likos et al., 2019; Lu and Likos, 2004).

Mixture theory and volume fraction concept

Let V be the volume of a representative elementary volume of the porous media which is assumed to be occupied by the solid skeleton, pore water, and pore air, and let V_s, V_w, and V_a be the volume of the solid, pore water and pore air, respectively. The volume fraction of the α phase for $\alpha=$ solid, water, and air is given by $\phi^\alpha=V_\alpha/V$, and thus

$$\phi^s+\phi^w+\phi^a=1. \tag{139}$$

Let ρ_α be the intrinsic density of phase α with $\alpha=s,w,a$, the density of the three-phase mixture reads,

$$\rho=\sum_{\alpha=s,w,a}\phi^\alpha\rho_\alpha=\sum_{\alpha=s,w,a}\rho^\alpha, \tag{140}$$

where $\rho^\alpha=\phi^\alpha\rho_\alpha$ is the partial density of phase α with $\alpha=s,w,a$. Let us define the degree of saturation of water ψ^w and the degree of saturation of air ψ^a as follows,

$$\psi^w=\frac{V_w}{V_w+V_a}=\frac{\phi^w}{1-\phi^s},\quad \psi^w=\frac{V_a}{V_w+V_a}=\frac{\phi^a}{1-\phi^s},\quad \psi^w+\psi^a=1. \tag{141}$$

Balance equations of linear momentum and mass

Based on the stress partition assumption, the total Cauchy stress tensor $\boldsymbol{\sigma}$ for the three-phase mixture is

$$\boldsymbol{\sigma}=\sum_{\alpha=s,w,a}\boldsymbol{\sigma}^\alpha, \tag{142}$$

where $\alpha=s,w,a$, and $\boldsymbol{\sigma}^\alpha=\phi^\alpha\boldsymbol{\sigma}_\alpha$ is the partial Cauchy stress tensor for the α phase in which $\boldsymbol{\sigma}_\alpha$ is the intrinsic Cauchy stress tensor of α phase. Assuming isotropic pore fluid pressures, the partial stress tensors for the pore fluid phase are

$$\boldsymbol{\sigma}^w=-\phi^w p_w\boldsymbol{I},\quad \boldsymbol{\sigma}^\alpha=-\phi^a p_a\boldsymbol{I}, \tag{143}$$

where p_w and p_a are intrinsic pore water pressure and pore air pressure, respectively, and $\boldsymbol{1}$ is the second-order identity tensor. It is noted that the above equation ignores the stress among the interface (e.g., the surface tension between pore water and pore air). Balance of the linear momentum for each phase can be written as

$$\nabla \cdot \boldsymbol{\sigma}^{\alpha} + \rho^{\alpha}\boldsymbol{g} + \boldsymbol{h}^{\alpha} = \rho^{\alpha}\frac{\mathrm{d}^{\alpha}\boldsymbol{v}_{\alpha}}{\mathrm{d}t}, \tag{144}$$

where $\boldsymbol{g}$ is the vector of gravity acceleration, $\boldsymbol{h}^{\alpha}$ is the resultant body force per unit current volume of the solid skeleton exerted on the α phase, ∇ is the gradient operator evaluated with respect to the current configuration, and the operator $\mathrm{d}^{\alpha}(\cdot)/\mathrm{d}t$ denotes a material time derivative following the α phase motion. Summation of (144) yields the balance of momentum for the whole mixture as

$$\nabla \cdot \boldsymbol{\sigma} + \rho\boldsymbol{g} = \sum_{\alpha=s,w,a} \rho^{\alpha}\frac{\mathrm{d}^{\alpha}\boldsymbol{v}_{\alpha}}{\mathrm{d}t}. \tag{145}$$

Fig. 14 shows the kinematics of three-phase porous media. For the mass balance equations of a three-phase mixture, the current configuration of the mixture is referred and the motions of the water and air phases are described following the motion of the solid skeleton in the current configuration. The balance of mass of each phase can be written as

$$\frac{\mathrm{d}\rho^{s}}{\mathrm{d}t} + \rho^{s}\nabla \cdot \boldsymbol{v} = 0, \tag{146}$$

$$\frac{\mathrm{d}\rho^{\alpha}}{\mathrm{d}t} + \rho^{\alpha}\nabla \cdot \boldsymbol{v} = -\nabla \cdot \boldsymbol{w}^{\alpha}, \quad \alpha = w, a, \tag{147}$$

where $\boldsymbol{w}^{\alpha} = \rho^{\alpha}\tilde{\boldsymbol{v}_{\alpha}}$ is the Eulerian relative flow vector of the α phase with respect to the solid matrix, $\tilde{\boldsymbol{v}}_{\alpha} = \boldsymbol{v}_{\alpha} - \boldsymbol{v}$ is the relative velocity of fluid α to the solid phase, and $\boldsymbol{v} = \boldsymbol{v}_s$. Assume a barotropic flow for each phase of the mixture (Malvern, 1969) and let the bulk modulus of the α phase by

$$K_{\alpha} = \rho_{\alpha}p_{\alpha}^{'}(\rho_{\alpha}), \quad \alpha = s, w, a, \tag{148}$$

where $p_{\alpha} = -\mathrm{tr}(\boldsymbol{\sigma}_{\alpha})$ is the intrinsic pressure acting on the α phase (Borja, 2006). Thus

$$\frac{\mathrm{d}\rho^{\alpha}}{\mathrm{d}t} = \rho_{\alpha}\left(\frac{\mathrm{d}\phi^{\alpha}}{\mathrm{d}t} + \frac{\phi^{\alpha}}{K_{\alpha}}\frac{\mathrm{d}p_{\alpha}}{\mathrm{d}t}\right). \tag{149}$$

Substituting (149) into (146) and (147) the balance of mass for each phase of the mixture becomes

$$\frac{\mathrm{d}\phi^{s}}{\mathrm{d}t} + \frac{\phi^{s}}{K_{s}}\frac{\mathrm{d}p_{s}}{\mathrm{d}t} + \phi^{s}\nabla \cdot \boldsymbol{v} = 0, \tag{150}$$

$$\frac{\mathrm{d}\phi^{\alpha}}{\mathrm{d}t} + \frac{\phi^{\alpha}}{K_{\alpha}}\frac{\mathrm{d}p_{\alpha}}{\mathrm{d}t} + \phi^{\alpha}\nabla \cdot \boldsymbol{v} = -\frac{1}{\rho_{\alpha}}\nabla \cdot \boldsymbol{w}^{\alpha}, \quad \alpha = w, a. \tag{151}$$

Taking the material time derivative of the void fractions of water and air in the direction of the solid phase motion and incorporating the mass balance of the solid skeleton yield

$$\frac{\mathrm{d}\phi^{\alpha}}{\mathrm{d}t} = (1-\phi^{s})\frac{\mathrm{d}\psi_{\alpha}}{\mathrm{d}t} + \psi^{\alpha}\left(\frac{\phi^{s}}{K_{s}}\frac{\mathrm{d}p_{s}}{\mathrm{d}t} + \phi^{s}\nabla \cdot \boldsymbol{v}\right), \quad \alpha = w, a. \tag{152}$$

Let K be the bulk modulus of the solid skeleton and it follows from the lines in Borja (2006) that

$$\phi^{s}\frac{\mathrm{d}p_{s}}{\mathrm{d}t} = -K\nabla \cdot \boldsymbol{v}. \tag{153}$$

It shall be noted that bulk modulus K represents the volumetric stiffness of the solid matrix while K_s as the intrinsic bulk modulus represents the volumetric stiffness of the solid itself. Substituting the above results into the balance of mass of water and air phase generates

$$(1-\phi^{s})\frac{\mathrm{d}\psi^{\alpha}}{\mathrm{d}t} + \frac{\phi^{\alpha}}{K_{\alpha}}\frac{\mathrm{d}p_{\alpha}}{\mathrm{d}t} + \psi^{\alpha}B\nabla \cdot \boldsymbol{v} + \frac{1}{\rho_{\alpha}}\nabla \cdot \boldsymbol{w}^{\alpha} = 0, \quad \alpha = w, a. \tag{154}$$

where $B = 1 - K/K_s$.

Internal energy balance and the effective stress concept

The rate change of internal energy of the three-phase mixture under isothermal conditions can be written as (e.g., Borja, 2006)

$$\rho\dot{\bar{e}} = \bar{\boldsymbol{\sigma}} : \boldsymbol{d} - s(1-\phi^s)\frac{\mathrm{d}\psi^w}{\mathrm{d}t} + \sum_{\alpha=w,a}\left(\frac{1}{\rho_\alpha}\nabla\cdot\boldsymbol{w}^\alpha - \phi^\alpha\nabla\tilde{v}_\alpha\right)p_\alpha + \sum_{\alpha=w,a}\frac{\phi^\alpha}{K_\alpha}\frac{\mathrm{d}p_\alpha}{\mathrm{d}t}p_\alpha, \tag{155}$$

where $\boldsymbol{d}$ is the rate of deformation tensor for the solid skeleton,

$$\begin{aligned}\bar{\boldsymbol{\sigma}} &= \boldsymbol{\sigma} + B\sum_{\alpha=w,a}\psi^\alpha p_\alpha \mathbf{1}\\ &= \boldsymbol{\sigma} + Bp_a\mathbf{1} - B\psi^w s\mathbf{1}\end{aligned} \tag{156}$$

is the effective stress on the solid skeleton, and $s = p_a - p_w$ is matric suction that is the difference between pore air pressure and pore water pressure in porous media (Israelachvili, 2011). Eq. (155) demonstrates that the effective stress tensor is a mechanical energy conjugate to the rate of the deformation of the solid skeleton. Mechanically, the effective stress is the portion of total stress imposed on the solid skeleton of a porous media. Note this article is focused on the single porosity theory for unsaturated geomaterials. For the double porosity theory, we refer to the literature (e.g., Barenblatt et al., 1960; Borja and Koliji, 2009; Choo and Borja, 2015; Nakshatrala et al., 2018).

References

Alonso, E.E., Gens, A., Josa, A., 1990. A constitutive model for partially saturated soils. Géotechnique 40 (3), 405–430.
Barenblatt, G.I., Zheltov, I.P., Kochina, I., 1960. Basic concepts in the theory of seepage of homogeneous liquids in fissured rocks [strata]. J. Appl. Math. Mech. 24 (5), 1286–1303.
Biot, M.A., 1941. General theory of three-dimensional consolidation. J. Appl. Phys. 12 (2), 155–164.
Bobaru, F., Foster, J.T., Geubelle, P.H., Silling, S.A., 2016. Handbook of Peridynamic Modeling. CRC Press.
Bobaru, F., Hu, W., 2012. The meaning, selection, and use of the peridynamic horizon and its relation to crack branching in brittle materials. Int. J. Fract. 176 (2), 215–222.
Borja, R.I., 2004. Cam-clay plasticity. part v: a mathematical framework for three-phase deformation and strain localization analyses of partially saturated porous media. Comput Methods Appl. Mech. Eng. 193 (48–51), 5301–5338.
Borja, R.I., 2006. On the mechanical energy and effective stress in saturated and unsaturated porous continua. Int. J. Solids Struct. 43 (6), 1764–1786.
Borja, R.I., 2013. Plasticity: Modeling & Computation. Springer Science & Business Media.
Borja, R.I., Koliji, A., 2009. On the effective stress in unsaturated porous continua with double porosity. J. Mech. Phys. Solids 57 (8), 1182–1193.
Borja, R.I., Song, X., Wu, W., 2013. Critical state plasticity. part vii: triggering a shear band in variably saturated porous media. Comput. Methods Appl. Mech. Eng. 261, 66–82.
Borja, R.I., Tamagnini, C., 1998. Cam-clay plasticity part iii: extension of the infinitesimal model to include finite strains. Comput. Methods Appl. Mech. Eng. 155 (1–2), 73–95.
Bowen, R.M., 1982. Compressible porous media models by use of the theory of mixtures. Int. J. Eng. Sci. 20 (6), 697–735.
Cao, J., Jung, J., Song, X., Bate, B., 2018. On the soil water characteristic curves of poorly graded granular materials in aqueous polymer solutions. Acta Geotech. 13 (1), 103–116.
Choo, J., Borja, R.I., 2015. Stabilized mixed finite elements for deformable porous media with double porosity. Comput. Methods Appl. Mech. Eng. 293, 131–154.
Coleman, B.D., Noll, W., 1974. The Thermodynamics of Elastic Materials with Heat Conduction and Viscosity. The Foundations of Mechanics and Thermodynamics. Springer, pp. 145–156.
Coussy, O., 2004. Poromechanics. John Wiley & Sons.
Coussy, O., 2011. Mechanics and Physics of Porous Solids. John Wiley & Sons.
Cowin, S.C., Doty, S.B., 2007. Tissue Mechanics. Springer Science & Business Media.
Cui, Y., Delage, P., 1996. Yielding and plastic behaviour of an unsaturated compacted silt. Géotechnique 46 (2), 291–311.
De Boer, R., 2000. Theory of Porous Media: Highlights in Historical Development and Current State. Springer Science & Business Media.
Dormieux, L., Kondo, D., Ulm, F.-J., 2006. Microporomechanics. John Wiley & Sons.
Foster, J.T., Silling, S.A., Chen, W.W., 2010. Viscoplasticity using peridynamics. Int. J. Numer. Methods Eng. 81 (10), 1242–1258.
Fredlund, D.G., Morgenstern, N.R., 1977. Stress state variables for unsaturated soils. J. Geotech. Geoenviron. Eng. 103 (ASCE 12919).
Fredlund, D.G., Rahardjo, H., 1993. Soil Mechanics for Unsaturated Soils. John Wiley & Sons.
Gallipoli, D., Gens, A., Sharma, R., Vaunat, J., 2003. An elasto-plastic model for unsaturated soil incorporating the effects of suction and degree of saturation on mechanical behaviour. Géotechnique 53 (1), 123–135.
Gens, A., 2010. Soil–environment interactions in geotechnical engineering. Géotechnique 60 (1), 3–74.
Gerstle, W., Sau, N., Silling, S., 2007. Peridynamic modeling of concrete structures. Nucl. Eng. Des. 237 (12–13), 1250–1258.
Gray, W.G., Miller, C.T., 2014. Introduction to the Thermodynamically Constrained Averaging Theory for Porous Medium Systems. Springer.
Gray, W.G., Miller, C.T., Schrefler, B.A., 2013. Averaging theory for description of environmental problems: what have we learned? Adv. Water Resour. 51, 123–138.
Holzapfel, G., 2000. Nonlinear Solid Mechanics: A Continuum Approach for Engineering Science. John Wiley & Sons Ltd, Chichester.
Houlsby, G., 1997. The work input to an unsaturated granular material. Géotechnique 47 (1), 193–196.
Israelachvili, J.N., 2011. Intermolecular and Surface Forces. Academic press.
Jabakhanji, R., Mohtar, R.H., 2015. A peridynamic model of flow in porous media. Adv. Water Resour. 78, 22–35.
Ji, B., Gao, H., 2004. Mechanical properties of nanostructure of biological materials. J. Mech. Phys. Solids 52 (9), 1963–1990.
Katiyar, A., Foster, J.T., Ouchi, H., Sharma, M.M., 2014. A peridynamic formulation of pressure driven convective fluid transport in porous media. J. Comput. Phys. 261, 209–229.
Khalili, N., Khabbaz, M., 1998. A unique relationship of chi for the determination of the shear strength of unsaturated soils. Géotechnique 48 (5).
Lai, X., Ren, B., Fan, H., Li, S., Wu, C., Regueiro, R.A., Liu, L., 2015. Peridynamics simulations of geomaterial fragmentation by impulse loads. Int. J. Numer. Anal. Methods Geomech. 39 (12), 1304–1330.
Lewis, R.W., Schrefler, B.A., 1998. The Finite Element Method in the Static and Dynamic Deformation and Consolidation of Porous Media. John Wiley.
Likos, W.J., Song, X., Xiao, M., Cerato, A., Lu, N., 2019. Fundamental challenges in unsaturated soil mechanics. In: Lu, N., Mitchell, J.K. (Eds.), Geotechnical Fundamentals for Addressing New World Challenges. Springer, pp. 209–236.
Lu, N., 2020. Unsaturated soil mechanics: fundamental challenges, breakthroughs, and opportunities. J. Geotech. Geoenviron. Eng. 146 (5), 02520001.
Lu, N., Godt, J.W., Wu, D.T., 2010. A closed-form equation for effective stress in unsaturated soil. Water Resour. Res. 46 (5).
Lu, N., Likos, W.J., 2004. Unsaturated Soil Mechanics. Wiley.
Lu, N., Likos, W.J., 2006. Suction stress characteristic curve for unsaturated soil. J. Geotech. Geoenviron. Eng. 132 (2), 131–142.

Lu, N., Mitchell, J.K., 2019. Geotechnical Fundamentals for Addressing New World Challenges. Springer.
Madenci, E., Oterkus, E., 2013. Peridynamic Theory and Its Applications. Springer Science & Business Media.
Malvern, L.E., 1969. Introduction to the Mechanics of a Continuous Medium.
Menon, S., Song, X., 2019. Coupled analysis of desiccation cracking in unsaturated soils through a non-local mathematical formulation. Geosciences (Basel) 9 (10), 428.
Nakshatrala, K.B., Joodat, S.H.S., Ballarini, R., 2018. Modeling flow in porous media with double porosity/permeability: mathematical model, properties, and analytical solutions. J. Appl. Mech. 85 (8), 081009.
Nikooee, E., Habibagahi, G., Hassanizadeh, S.M., Ghahramani, A., 2013. Effective stress in unsaturated soils: a thermodynamic approach based on the interfacial energy and hydromechanical coupling. Transp. Porous. Media 96 (2), 369–396.
Nova, R., Castellanza, R., Tamagnini, C., 2003. A constitutive model for bonded geomaterials subject to mechanical and/or chemical degradation. Int. J. Numer. Anal. Methods Geomech. 27 (9), 705–732.
Nuth, M., Laloui, L., 2008. Effective stress concept in unsaturated soils: clarification and validation of a unified framework. Int. J. Numer. Anal. Methods Geomech. 32 (7), 771–801.
Ouchi, H., Katiyar, A., York, J., Foster, J.T., Sharma, M.M., 2015. A fully coupled porous flow and geomechanics model for fluid driven cracks: a peridynamics approach. Comput. Mech. 55 (3), 561–576.
Parks, M.L., Lehoucq, R.B., Plimpton, S.J., Silling, S.A., 2008. Implementing peridynamics within a molecular dynamics code. Comput. Phys. Commun. 179 (11), 777–783.
Silling, S., 2004. Emu Users Manual. Sandia National Laboratories, Albuquerque.
Silling, S., Littlewood, D., Seleson, P., 2015. Variable horizon in a peridynamic medium. J. Mech. Mater Struct. 10 (5), 591–612.
Silling, S.A., 2000. Reformulation of elasticity theory for discontinuities and long-range forces. J. Mech. Phys. Solids 48 (1), 175–209.
Silling, S.A., 2014. Origin and effect of nonlocality in a composite. J. Mech. Mater Struct. 9 (2), 245–258.
Silling, S.A., 2017. Stability of peridynamic correspondence material models and their particle discretizations. Comput. Methods Appl. Mech. Eng. 322, 42–57.
Silling, S.A., Askari, E., 2005. A meshfree method based on the peridynamic model of solid mechanics. Comput. Struct. 83 (17–18), 1526–1535.
Silling, S.A., Epton, M., Weckner, O., Xu, J., Askari, E., 2007. Peridynamic states and constitutive modeling. J. Elast. 88 (2), 151–184.
Silling, S.A., Lehoucq, R., 2010. Peridynamic theory of solid mechanics. Advances in Applied Mechanics, 44. Elsevier, pp. 73–168.
Simo, J.C., Hughes, T.J., 1999. Computational Inelasticity, 7. Springer Science & Business Media.
Song, X., 2017. Transient bifurcation condition of partially saturated porous media at finite strain. Int. J. Numer. Anal. Methods Geomech 41 (1), 135–156.
Song, X., Borja, R.I., 2014. Finite deformation and fluid flow in unsaturated soils with random heterogeneity. V Top Vadose Zone J. 13 (5).
Song, X., Borja, R.I., 2014. Mathematical framework for unsaturated flow in the finite deformation range. Int. J. Numer. Methods Eng. 97 (9), 658–682.
Song, X., Khalili, N., 2019. A peridynamics model for strain localization analysis of geomaterials. Int. J. Numer. Anal. Methods Geomech. 43 (1), 77–96.
Song, X., Menon, S., 2018. Modeling of chemo-hydromechanical behavior of unsaturated porous media: a nonlocal approach based on integral equations. Acta Geotech. 1–21.
Song, X., Wang, M.-C., 2019. Molecular dynamics modeling of a partially saturated clay-water system at finite temperature. Int. J. Numer. Anal. Methods Geomech. 43 (13), 2129–2146.
Song, X., Wang, K., Bate, B., 2018. A hierarchical thermo-hydro-plastic constitutive model for unsaturated soils and its numerical implementation. Int. J. Numer. Anal. Methods Geomech 42 (15), 1785–1805.
Song, X., Wang, K., Ye, M., 2018. Localized failure in unsaturated soils under non-isothermal conditions. Acta Geotech 13 (1), 73–85.
Song, X., Ye, M., Wang, K., 2017. Strain localization in a solid-water-air system with random heterogeneity via stabilized mixed finite elements. Int. J. Numer. Methods Eng. 112 (13), 1926–1950.
Stakgold, I., Holst, M.J., 2011. Green's Functions and Boundary Value Problems, 99. John Wiley & Sons.
Sulem, J., Vardoulakis, I., 1995. Bifurcation Analysis in Geomechanics. CRC Press.
Terzaghi, K., Peck, R.B., Mesri, G., 1996. Soil mechanics in Engineering Practice. John Wiley & Sons.
Turner, D.Z., 2013. A non-local model for fluid-structure interaction with applications in hydraulic fracturing. Int. J. Comput. Methods Eng. Sci. Mech. 14 (5), 391–400.
Van Genuchten, M.T., 1980. A closed-form equation for predicting the hydraulic conductivity of unsaturated soils. Soil Sci. Soc. Am. J. 44 (5), 892–898.
Wang, K., Song, X., 2020. Strain localization in non-isothermal unsaturated porous media considering material heterogeneity with stabilized mixed finite elements. Comput. Methods Appl. Mech. Eng 359 (2), 1–33.
Warren, T.L., Silling, S.A., Askari, A., Weckner, O., Epton, M.A., Xu, J., 2009. A non-ordinary state-based peridynamic method to model solid material deformation and fracture. Int. J. Solids Struct. 46 (5), 1186–1195.
Wheeler, S., Sivakumar, V., 1995. An elasto-plastic critical state framework for unsaturated soil. Géotechnique 45 (1), 35–53.
Zienkiewicz, O.C., Chan, A., Pastor, M., Schrefler, B., Shiomi, T., 1999. Computational Geomechanics with Special Reference to Earthquake Engineering. Wiley.